Bridging Information-Theoretic and Geometric Compression in Language Models

Emily Cheng and **Corentin Kervadec**
Universitat Pompeu Fabra / Barcelona
{name.lastname}@upf.edu

Marco Baroni
ICREA / Barcelona
marco.baroni@upf.edu

Abstract

For a language model (LM) to faithfully model human language, it must compress vast, potentially infinite information into relatively few dimensions. We propose analyzing compression in (pre-trained) LMs from two points of view: geometric and information-theoretic. We demonstrate that the two views are highly correlated, such that the intrinsic geometric dimension of linguistic data predicts their coding length under the LM. We then show that, in turn, high compression of a linguistic dataset predicts rapid adaptation to that dataset, confirming that being able to compress linguistic information is an important part of successful LM performance. As a practical byproduct of our analysis, we evaluate a battery of intrinsic dimension estimators for the first time on linguistic data, showing that only some encapsulate the relationship between information-theoretic compression, geometric compression, and ease-of-adaptation.

1 Introduction

To speak a language is not to memorize all possible utterances, but to instead extract the finite ruleset and lexicon that generates them (Chomsky, 1986). That is, language, though nominally high-dimensional, can be compressed to a comparatively small *intrinsic dimension*.

The recent success of *(large) language models* demonstrates that artificial neural networks, too, can acquire linguistic knowledge. Current language models (LMs) are Transformer-based architectures at-scale (Vaswani et al., 2017) that are trained on the conditional distribution of natural language (OpenAI, 2023; Zhang et al., 2022; Touvron et al., 2023; Chowdhery et al., 2022) and that are inching closer to human-like linguistic robustness (Brown et al., 2020; Liang et al., 2022; Wang et al., 2019b). For an LM to faithfully model language, it must encode linguistic training data into finitely many variables that allow generalization to infinitely many grammatical utterances. That is, it must perform a successful form of data compression.

Thus, following the line of research that aims to better understand LM behavior (Wei et al., 2022; Zhang et al., 2021; Rogers et al., 2020), in this work we provide initial insights on how they *compress linguistic knowledge*. We demonstrate an empirical link between two types of compression: geometric and information-theoretic. In particular, we ask: how, and by how much, do LMs compress linguistic data? Furthermore, what are linguistic correlates to compressibility? Is compression a good predictor of rapid adaptation? We show that (1) intrinsic dimension (ID) of linguistic data representations under an LM tracks information-theoretic coding length; (2) greater data compression predicts ease-of-adaptation in causal language modeling tasks; (3) interpretable linguistic properties such as vocabulary size and syntactic structure modulate ID; and (4) different model sizes recover similar ranges of ID. Finally, as a practical contribution, (5) we explore different ways to estimate ID of linguistic data, and find only some to capture the relation between ID, coding length, and ease-of-adaptation.

2 Related Work

Causal Language Models State-of-the-art language models are based on the Transformer architecture (Vaswani et al., 2017), which consists of alternating feed-forward and self-attention modules (Bahdanau et al., 2015). They are trained using *self-supervised learning* on sequences of *tokens*, where a token is defined as the atomic unit (e.g., a word or a sub-word) fed into the language model. Due to their current ubiquity, we focus on autoregressive models trained on a *causal language modeling* objective, that is, next token prediction given a context of previous tokens (Brown et al., 2020; Radford and Narasimhan, 2018; Zhang et al., 2022).

Language models are typically measured against human performance on linguistic benchmarks.

Proceedings of the 2023 Conference on Empirical Methods in Natural Language Processing, pages 12397–12420
December 6-10, 2023 ©2023 Association for Computational Linguistics

Evaluation may be done post-finetuning or in a low-shot regime, where the model completes a linguistic task given few or zero examples. A variety of benchmarks, such as GLUE (Wang et al., 2019b), SuperGLUE (Wang et al., 2019a), and BigBENCH (Srivastava et al., 2022) have been proposed, evaluating, for instance, model performance on textual entailment, question-answering, semantic equivalence, or sentiment analysis. Indeed, human baselines for GLUE and SuperGLUE have already been surpassed by LMs that contain billions of parameters (e.g., PaLM 540B (Chowdhery et al., 2022)).

2.1 Compression in LMs

There is a wide body of work analyzing compression in deep neural architectures. In statistical learning theory, compression has been empirically and theoretically linked to generalization (Shwartz-Ziv and Tishby, 2017; Arora et al., 2018). Moreover, deep learning models are thought to minimize description length (Perez et al., 2021; Voita and Titov, 2020; Blier and Ollivier, 2018). In large LMs, implicit compression of neural network parameters has been linked to ease-of-finetuning and generalization (Aghajanyan et al., 2021). Our work complements this line of research by focusing on compression of *data representations* rather than network parameters. We consider compression from two different perspectives: information-theoretic and geometric (intrinsic dimension).

Information-theoretic compression Compression in neural networks can be quantified from an information-theoretic point of view (Shannon, 1948). For instance, the *information plane* (IP), a widely studied framework introduced by Shwartz-Ziv and Tishby (2017) and Tishby and Zaslavsky (2015), quantifies compression per-layer as the mutual information between representations and inputs. However, there is little consensus in the relevant literature on the appropriate estimator to measure this *internal* compression of inputs (Saxe et al., 2018; Goldfeld et al., 2019; Noshad et al., 2019; Chelombiev et al., 2019; Geiger, 2022).

Instead, as probabilistic models, LMs are natural *black-box* compressors: the negative log-likelihood of the next token given context is, by definition, its Shannon coding length in bits (Shannon, 1948). Concurrent work explores the equivalence between self-supervised prediction and lossless compression, demonstrating that LMs can be powerful general-purpose compressors (Delétang et al., 2023). We similarly focus on *information-theoretic coding length* of inputs under a pre-trained model, which is a simple measure of compression that, to our knowledge, has not been shown to be analytically equivalent to geometric compression. We develop this measure further in section 3.2.

Intrinsic Dimension (ID) *Geometric* compression is commonly quantified using dimensionality reduction techniques. Often underlying these approaches is the manifold learning hypothesis (Goodfellow et al., 2016), or the notion that real-life, high-dimensional data often lie on a low-dimensional manifold. Intrinsic dimension (ID), or the number of degrees of freedom in the data, is the dimension of this data manifold.

Perhaps the most prototypical ID estimators are linear projective methods like random projection (Li et al., 2018) or Principal Component Analysis (PCA) (Jolliffe, 1986). While these project data to a *linear* subspace, the underlying geometric object need not be linear; therefore, e.g., PCA poorly estimates ID for curved manifolds (Campadelli et al., 2015). Nonlinear ID estimators include Correlation Dimension (Grassberger and Procaccia, 1983); Fisher Separability (Albergante et al., 2019); and a host of “nearest-neighbor" (NN)-based methods, which use the fact that manifolds look locally Euclidean to fit the ID based on local neighbor distributions (Facco et al., 2017; Levina and Bickel, 2004; Haro et al., 2008; Amsaleg et al., 2018). Such methods outperform linear ones on ID estimation benchmarks (Campadelli et al., 2015). In section 4, we will assess these methods in the context of linguistic data, and analyze how each of them relates to coding length and ease-of-adaptation.

In deep learning, there has been recent interest in using ID to characterize learning complexity. Intrinsic dimension has been quantified for neural network parameters (Li et al., 2018), as well as for input data and their representations in visual and protein-sequence domains (Cohen et al., 2020; Recanatesi et al., 2019; Ansuini et al., 2019; Valeriani et al., 2023; Pope et al., 2021). These studies show that deep neural architectures learn low-dimensional structures, encoding parameter weights and training data into orders-of-magnitude lower ID than their ambient dimension.

In the linguistic domain, low ID of LM *parameters* has been shown to underlie efficient task adaptation (Aghajanyan et al., 2021), where optimization occurs in low-dimensional, task-specific subspaces (Zhang et al., 2023). Moreover, parameter redundancy in pre-trained LMs can be exploited to design parameter-efficient finetuning methods such as LoRA (Hu et al., 2022). We are interested in ID of *data representations* as opposed to *LM parameters*, as (1) we want to study how different linguistic properties affect their coding; (2) ID estimation of model parameters can be expensive– large LMs can have billions of parameters, while input representations are lower-dimensional, e.g., $D = 4096$ in OPT-6.7b (Zhang et al., 2022). In related work on LM *representation* ID, contextual word embeddings have been found to lie in low-dimensional linear subspaces (Mamou et al., 2020; Hernandez and Andreas, 2021). Most similar to our work, Cai et al., 2021 show that Transformer embeddings of the Wikitext and Penn TreeBank datasets constitute nonlinear manifolds of ID $\sim \mathcal{O}(10)$.

3 Methods

Our work attempts to bridge notions of geometric and information-theoretic compression of linguistic data under an LM, and subsequently relate these to ease-of-adaptation. We do so by quantifying the ID of data representations, information-theoretic coding length of linguistic inputs under an LM, and ease-of-finetuning in order to determine whether these three phenomena are correlated.

Notation Let a linguistic dataset $X = \{x^{(i)}\}_{i=1}^{N}$ consist of N sequences of tokens, where each sequence $x^{(i)}$ has length $l(x^{(i)})$. Let $\mathcal{M}$ be a (pre-trained) causal language model described by $p_{\mathcal{M}}(\cdot|x_{<j})$, the conditional probability distribution of the j^{th} token given its past context of tokens.

Models & Datasets Experiments are performed for the product of models $\mathcal{M} \in$ [OPT-350m, OPT-1.3b, OPT-6.7b] and datasets $X \in$ table 1. We focus on OPT suite of causal language models due to their accessibility (Zhang et al., 2022). For the datasets, we start from a list of corpora including the GLUE and SuperGLUE benchmarks, then pick those whose size is large enough for ID estimates to converge ($N \geq 10000$). Then, for computational efficiency, we randomly subsample each dataset to size $N' = \max(N, 50000)$, where 50000 is chosen conservatively based on preliminary analyses of convergence of bootstrapped ID estimates (see appendix A.2).

In addition to external datasets, we create one baseline dataset per model, which we call OPTCorpus, of ~ 24 million tokens by repeatedly randomly sampling from $\mathcal{M}$ until `[EOS]` is reached. The conditional next-token distribution of OPTCorpus approximates that of $\mathcal{M}$ so to serve as a reference datapoint.

Benchmark	Datasets
GLUE	cola, mnli, mrpc, qnli qqp, rte, sst2, stsb
SuperGLUE	boolq, multirc, wic
	IMDB, Penn Treebank, Bookcorpus, Wikitext fr, Tweets, Pile-10k, CNN Dailymail, Openwebtext-10k, CONCODE, OPTCorpus, OPTCorpus-permuted, OPTCorpus-swapped, OPTCorpus-random, Wikitext, Wikitext-permuted, Wikitext-swapped, Wikitext-random

Table 1: List of datasets used in experiments. We use all datasets for ID and PPL estimation and the ones in the last block for finetuning (except for OPTCorpus, which already reflects the distribution of the model).

In order to determine the effects of syntax and lexical semantics on compression, we define three transformations which we apply to a *dataset*: (1) *dataset-permuted:* for each sequence in *dataset*, randomly permute its tokens. This ablates syntax to retain bag-of-tokens lexical information. (2) *dataset-swapped*: excluding special tokens, create a random permutation σ over the vocabulary. For each sequence in *dataset*, deterministically map each token by σ. This ablates lexical patterns, retaining syntactic structure. (3) *dataset-random*: randomly replace each token in *dataset* with another (excluding special tokens). This ablates both syntactic and lexical structure.

Notably, several shallow linguistic descriptors are preserved with these transformations: dataset size, sequence length and vocabulary size (1-3), vocabulary entropy (1,2), and token frequency (1). We apply the transformations to OPTCorpus and wikitext, producing six additional datasets.

3.1 Intrinsic Dimension

Given model $\mathcal{M}$ and dataset X, we estimate the representational ID of X under $\mathcal{M}$ as follows (see also fig. 1):

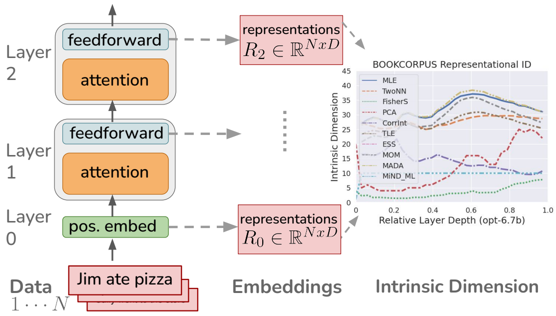

Figure 1: ID estimation. Data (bottom left) are fed into an LM with M blocks (left). Activations post-embedding/[feedforward, attention] blocks $i = 1 \cdots M$ are extracted and aggregated across the sequence length to produce an $N \times D$ dimensional matrix of representations R_i. Then, the ID of each R_i is estimated to produce an ID "profile" (right plot).

1. **Preprocess data.** Let the context window length of $\mathcal{M}$ be $l_{\mathcal{M}}$. We preprocess X by splitting all $x^{(i)}$ with length $l^{(i)} > l_{\mathcal{M}}$ into sequences with maximum length $l_{\mathcal{M}}$.
2. **Gather representations.** Evaluate $\mathcal{M}(X)$, gathering intermediate representations after contextualized embedding and after each attention+feed-forward block. In particular, representations are extracted after the residual connection and LayerNorm.
3. **Aggregate representations.** Because input sequences $x^{(i)}$ are variable-length, we use the vector associated to the last token of each layer to represent it. Due to auto-regressive self-attention, the last token in the sequence is the only one to incorporate information from all other tokens in the sequence. Moreover, in the context of causal language modeling, the last token representation is the one used for next-token prediction in the top layer of the model, so it is the one where all information relevant to the prediction task should be concentrated. We leave testing alternative aggregation strategies, such as average pooling (cf. Valeriani et al., 2023) to future work.

   After the aggregation step, we have dataset representations

   $$\mathbf{R} := \{R_j\}_{j=1}^{M}; R_j \in \mathbb{R}^{N \times D},$$

   where D, the hidden dimension of the model, is the ambient (extrinsic) dimension of data representations, and $\mathcal{M}$ has M layers.
4. **Estimate ID.** Per layer j, compute the ID d_j of R_j using ID estimator $g : \mathbb{R}^{N \times D} \to \mathbb{Z}_+; R_j \mapsto d_j$.

We test 12 different ID estimators g, grouping them into categories based on technique: nine NN-based (Facco et al., 2017; Farahmand et al., 2007; Carter et al., 2010; Amsaleg et al., 2019, 2018; Haro et al., 2008; Johnsson et al., 2015; Rozza et al., 2012; Ceruti et al., 2014), one projective (PCA), one based on fine-grained clustering (Fisher Separability, Albergante et al., 2019), and one fractal-based (Correlation Dimension, Grassberger and Procaccia, 1983). Further details on estimators can be found in appendix A.1. We implement all estimators using the `skdim` Python package (Bac, 2020).

3.2 Information-Theoretic Compression

Information-theoretic compression is directly related to the training objective of the model, which minimizes the average negative log-likelihood loss of next-token prediction over the training set.

Learning minimizes coding length The average negative log-likelihood (NLL) training objective of causal LMs is given by

$$\min_{\theta} \frac{1}{\sum_{i=1}^{N} l(x^{(i)})} \sum_{i=1}^{N} \sum_{j=1}^{l(x^{(i)})} -\log p_{\mathcal{M}}(x_j^{(i)} | x_{<j}^{(i)}; \theta), \tag{1}$$

that is, to minimize the empirical negative log-likelihood of the next token given its context with respect to model parameters θ. This is analytically equivalent to minimizing the average number of bits to encode the j^{th} token under $p_{\mathcal{M}}$.

We are interested in quantifying information-theoretic compression at the sequence level. We do so by using perplexity, a common metric in NLP.

Perplexity The perplexity (PPL) of a sequence $x^{(i)}$ is the exponentiated negative log-likelihood loss

$$PPL^{(i)} := 2^{\frac{1}{l(x^{(i)})} \sum_{j=1}^{l(x^{(i)})} -\log p_{\mathcal{M}}(x_j^{(i)} | x_{<j}^{(i)}; \theta)}. \tag{2}$$

We compute the average PPL for each dataset X by performing forward passes through $\mathcal{M}$. As PPL is monotonic in coding length, we use PPL as our measure of interest to proxy information-theoretic compression, later relating this quantity to the representational ID of X.

3.3 Ease-of-Adaptation

Low ID of pre-trained LM parameters has been shown to predict ease-of-finetuning (Aghajanyan et al., 2021). We complement this finding by correlating the ID of *data representations* to an LM's ease-of-adaptation to that dataset.

Ease-of-adaptation to a downstream task depends not only on the inputs X but also on task-specific outputs. For instance, binary classification can be less complex than causal language modeling given the same inputs X. As it is not always clear what is the best way to encode the outputs in order to measure the quantities of our interest, we focus on adaptation under a causal language modeling objective, which is the same as the model's pre-training objective. This entails little loss of generality, as task adaptation is nowadays commonly framed as a language model adaptation problem.

Adaptation procedure We perform finetuning for each of OPT-350m, 1.3b, and 6.7b on the datasets X in table 1 that are suited to causal language modeling, i.e., omitting [Super]GLUE.

Due to resource constraints, and as we compare between datasets and not models, we perform full finetuning for OPT-350m and finetune using LoRA (Hu et al., 2022) for the larger sizes. We end finetuning at a maximum of 15 epochs or when validation loss converges. Loss is considered to have converged as soon as it fails to decrease for 3 evaluation steps, each 500 iterations apart. Detailed hyperparameter settings may be found in appendix C.

Adaptation metrics We quantify ease-of-adaptation with the following, where T is defined as the number of iterations until convergence:

1. PPL_T: final evaluation perplexity.
2. Sample complexity $S = \frac{1}{T}\sum_{t=1}^{T} PPL_t$, where PPL_t is the evaluation PPL at evaluation step t.

Finally, we compute Spearman correlations between these metrics, zero-shot perplexity (PPL_0), and ID to assess whether the two types of compression and ease-of-adaptation are linked.

4 Results

We find that, similar to protein models and visual networks (Ansuini et al., 2019; Valeriani et al., 2023), the ID of linguistic data representations is significantly lower than their ambient dimension: in our case, by roughly 2 orders of magnitude. In particular, while the ambient dimension of representations in OPT-350m, OPT-1.3b, and OPT-6.7b are $D = 1024$, 2048, and 4096, respectively (Zhang et al., 2022), dataset representational ID is $d = \mathcal{O}(10)$, see fig. 5.

For simplicity, in the main article we present results on one representative NN-based estimator, the Expected Simplex Skewness (ESS) method of Johnsson et al., 2015, as it is the only one to significantly correlate with all other estimators ($\alpha = 0.1$) (see fig. 6).[1] We present results on other estimators in appendix E, and we comment on other (non-NN-based) ID estimators in section 4.4. Also for practicality, we report in the main article results obtained with one model, OPT-6.7b, only commenting on other models when relevant, and one aggregated ID measure across layers: the *max* ID value, seen as a conservative upper bound on ID across layers. This choice is supported by the observation that, for most datasets, the ID profile over layers is quite flat (appendix D). Results with other aggregated measures are presented in appendix E.

Our primary result is that, in the pre-trained LMs tested, information-theoretic compression (PPL) predicts geometric compression (ID), and low ID predicts ease-of-adaptation. We then take a closer look at which linguistic attributes of a dataset predict its ID, finding that not only several shallow linguistic descriptors but also grammatical and lexical structure enable geometric compression. Finally, we find that, qualitatively, ID tends to be stable across model sizes and types , and comment on the differences between ID estimators.

4.1 ID tracks information-theoretic compression

Information-theoretic and geometric description length of data under OPT are Spearman-correlated. As shown for OPT-6.7b in fig. 2a, data PPL predicts ID, $\rho = 0.51$ ($p = 0.01$). The significant positive correlation between PPL and ID, moreover, holds for all model sizes tested: $\rho = 0.66$, $p < 0.01$ for OPT-350m and $\rho = 0.49$, $p = 0.01$ for OPT-1.3b, the correlation being most salient for the smallest model (see figs. E.3a and E.3d). We hypothesize that model optimization in higher dimensions permits discovery of better representa-

[1] We also experimented with ensembling ID metrics, but found the various ensembling methods hard to justify as NN-based estimators are very over-represented in our panel.

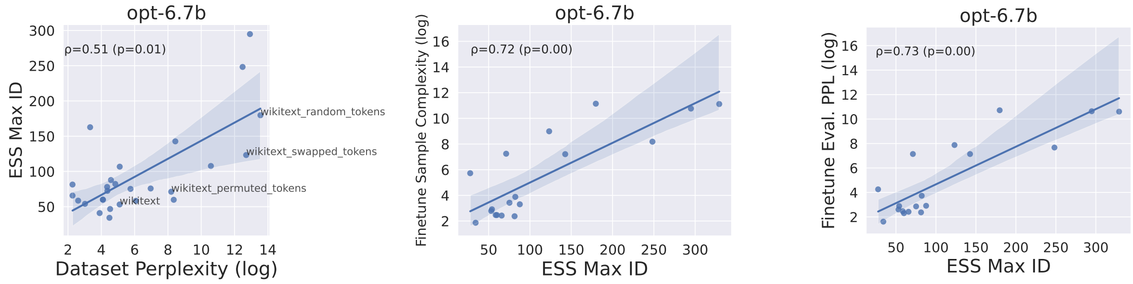

(a) Intrinsic dimension (ESS max ID) vs. data perplexity (log-PPL).

(b) Sample complexity vs. Intrinsic dimension (ESS max ID)

(c) Final log-PPL vs. Intrinsic dimension (ESS max ID).

Figure 2: Intrinsic dimension is significantly positively correlated to (a) dataset PPL ($p = 0.01$); and also predicts ease-of-adaptation metrics (b) sample complexity ($p < 0.01$) and (c) final evaluation PPL ($p < 0.01$). Both ID and dataset perplexity in (a) are measured before finetuning; in (b) and (c), ID is measured before finetuning and the y-axes after finetuning.

tions in d-dimensional intrinsic space, as evidenced by the correlation between performance and model size in LM scaling laws. Then, on a given dataset, larger model sizes may encounter an ID floor effect, thus weakening the correlation between PPL and ID compared to smaller sizes.

4.2 Compression is linked to Ease-of-Adaptation

As evidenced by the positive trends in figs. 2b and 2c, ID predicts sample complexity ($\rho = 0.72$, $p < 0.01$) as well as final PPL after convergence ($\rho = 0.73$, $p < 0.01$). These trends, moreover, are robust to model size: ID predicts sample complexity at $\rho = 0.61$, $p = 0.01$ for OPT-1.3b and $\rho = 0.81$, $p = 0.01$ for OPT-350m (figs. E.3b and E.3e); and ID predicts final PPL after finetuning at $\rho = 0.65$, $p < 0.01$ for OPT-1.3b and $\rho = 0.81$, $p = 0.01$ for OPT-350m (figs. E.3c and E.3f).

Results indicate that data which are more compressed zero-shot under the LM are easier to adapt to. Moreover, they corroborate findings in Aghajanyan et al., 2021, in which low *parameter* ID in pre-trained LMs predicts rapid adaptation. We hypothesize that this is because intrinsic data rank bottlenecks intrinsic parameter rank and vice-versa (see Rozza et al., 2012 for discussion).

4.3 Linguistic Correlates to Compression

In pre-trained OPT, geometric compression can be explained partially by data perplexity. But, taking a closer look, ID also correlates with interpretable linguistic descriptors such as syntactic structure or token entropy.

	V	$\mathcal{H}_V$	$\tilde{L}$	N_{tok}
Max ID	0.50 p=0.01	0.44 p=0.02	0.15	0.15

Table 2: For OPT-6.7b, Spearman correlations ρ between ESS max ID and dataset vocabulary size (V), vocabulary entropy ($\mathcal{H}_V$), average sequence length $\tilde{L}$, and size in tokens N_{tok}. Significant correlations at $\alpha = 0.05$ are displayed with the corresponding p-value.

Linguistic Structure Permits Compression Ablating linguistic structure increases ID and perplexity of data representations. This may be seen in fig. 2a for OPT-6.7b, where both the ID and perplexity of the permuted, swapped, and random variants increase with respect to the baseline for the wikitext dataset. Moreover, this relationship holds for all model sizes, see figs. E.3a and E.3d, and generally for other ID estimators, see appendix E. This indicates that learned grammatical and lexical structure permits compression in LMs; furthermore, the small increase in ID from wikitext to wikitext-permuted compared to other variants suggests that bag-of-words lexical semantics, rather than complex syntactic structure, accounts for much of geometric compression. Interestingly, this ties in with general estimates of the relative information load of syntax and lexical semantics in human language (Mollica and Piantadosi, 2019).

Some Shallow Linguistic Descriptors Predict ID but Are Uncorrelated to Perplexity Beyond linguistic structure, two related shallow linguistic descriptors also predict ID: vocabulary size V (number of unique tokens in the dataset) and vocabulary entropy $\mathcal{H}_V$ (Shannon entropy of token frequency

Figure 3: Example evolution of ID (ESS) over layers for three tasks (left to right): wikitext, sst2, and tweets. In general, ID profiles can be dissimilar for different datasets under the same model, and ID profiles for OPT-350m, 1.3b, and 6.7b appear correlated, with larger extrinsic dimension lending itself to slightly (not proportionately) larger intrinsic dimension.

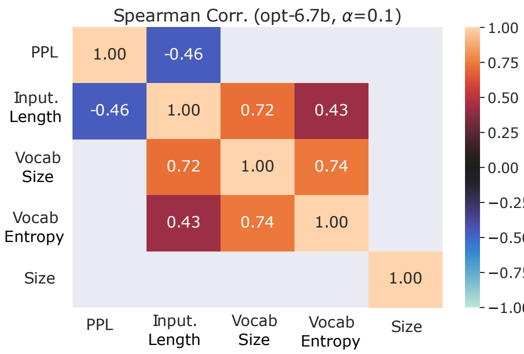

Figure 4: Spearman correlations between data descriptors: information-theoretic descriptor PPL (top/left), and shallow linguistic descriptors (bottom/right); only correlations significant at $\alpha = 0.1$ shown. Shallow metrics highly correlate to each other but not to PPL.

in the dataset), see Table 2. In contrast, average sequence length (in tokens) $\tilde{L}$ and dataset size (in tokens) N_{tok} do not predict ID.[2]

That descriptors such as vocabulary size and entropy predict ID is intuitive: with, e.g., a larger vocabulary, more information needs to be encoded. Furthermore, as expected, these descriptors are correlated to one another. However, the descriptors are *not positively correlated* to PPL (fig. 4), suggesting that the relationship between information-theoretic and geometric compression is not explained by shallow dataset properties.

The relation between shallow linguistic descriptors and ID generally holds across model size and ID estimators; see appendix E for further discussion, extending to other layer-aggregate measures of ID.

[2]It is crucial that the dataset be big enough to prevent spurious correlations between size and ID due to scaling effects (see appendix A.2).

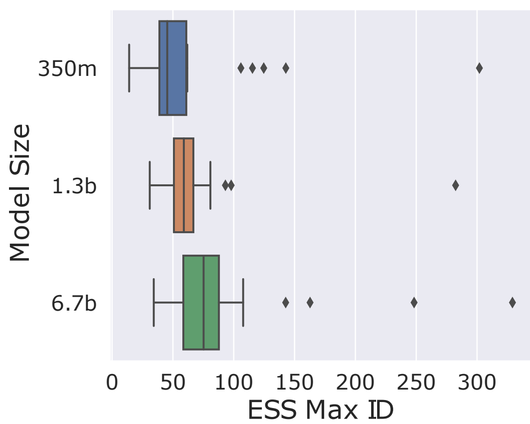

Figure 5: Distributions of max ID (aggregated over layers of the Transformer) across tasks, computed using the ESS estimator. Despite the model extrinsic dimension doubling (ED = 1024, 2048, 4096 from top to bottom), the ID remains fairly stable. Apart from a few outliers, the max ID over layers is less than 100, that is, all IDs computed over all layers are generally $\mathcal{O}(10)$.

4.4 Intrinsic Dimension of Representations

We have presented ID as it relates to information-theoretic compression and ease-of-adaptation; now we address the question of geometric compression itself. First, we show that the various models compress data into similar ranges of ID *regardless of extrinsic hidden dimension*, lending weight to the manifold hypothesis for linguistic data. We further report on how ID estimation with different methods produces a complicated picture, and we comment on results evaluated on the full battery of 12 estimators.

Different model size, similar ID We find that all tested models compress data to a similar range of ID, around $\mathcal{O}(10)$. Although the model hidden dimension doubles from OPT-350m to 1.3b to 6.7b, the range of data representational ID does not sig-

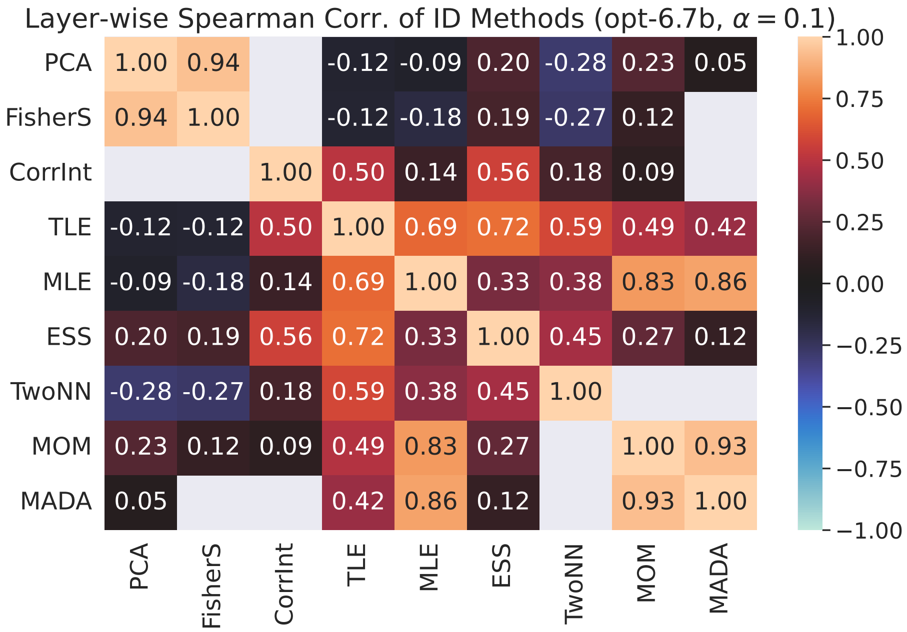

Figure 6: Spearman correlations between ID metrics: the bottom-right block of correlated metrics correspond to NN-based methods, while the top-left are PCA, Fisher Separability, and Correlation Dimension, respectively a linear projective, fine-grained clustering, and fractal method.

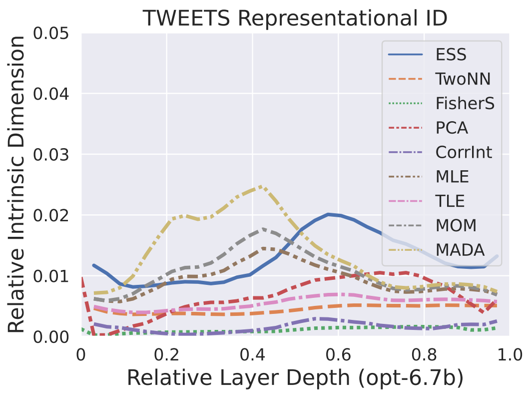

Figure 7: Different ID methods' relative ID estimates (= ID / ED) over layers in OPT-6.7b for the Tweets dataset. While some groups of methods are correlated, they produce different ID profiles for the same data.

nificantly change, see fig. 5.

Moreover, the *evolution* of ID across the layers of different model sizes follows similar trajectories: qualitatively, for all tasks, the OPT models' ID profiles follow similar global patterns (e.g., similar number of peaks), with larger models having slightly larger intrinsic dimension, see examples in fig. 3. For extended discussion of ID evolution across layers, see appendix D.

Similar ID values and evolution across different models echo results in the visual domain (Ansuini et al., 2019) and evidence the manifold hypothesis for linguistic data. Together with past work, our results suggest that different-sized (but similar-performing) models which are trained on the same data and objective can independently recover the latent dimension of data and exhibit similar patterns of processing.

ID estimators aren't equal; some are useful Though ID estimators based on similar analytical methods are correlated (fig. 6), different ID estimators can produce different ID profiles for the same dataset (e.g., fig. 7). This can stem from a number of factors pertaining to assumptions and analytical method. For instance, we find the NN-based methods to be most predictive of data perplexity and ease-of-adaptation, and PCA and Fisher Separability to be least predictive. This may be because (1) PCA assumes that the underlying data manifold is linear, which may lead to poor ID estimation (consider a 1D line embedded in 2D space; PCA will estimate an ID of 2 as there are two principal directions of variance); (2) Fisher Separability systematically underestimates ID for non-uniformly distributed data (Albergante et al., 2019), and Transformer representations are highly anisotropic (Cai et al., 2021). Lastly, among the 12 estimators tested, we could not produce sensible results for three of them (Rozza et al., 2012; Ceruti et al., 2014; Carter et al., 2010), see appendix A.3 for discussion.

While we cannot claim that any single estimator produces the "true" ID, it appears that, for purposes of ID estimation of linguistic datasets as encoded in LMs, NN-based methods are the most *useful* ones, being reliable predictors of information-theoretic compression and ease-of-adaptation (appendix E). More generally, the differing results obtained with various ID estimators reveal a need to validate them against linguistic data, which may violate underlying assumptions of common estimators, such as the global isotropy assumption in Fisher Separability (Albergante et al., 2019). While there indeed exist ID estimation benchmarks for synthetic manifolds and image data, and while NN-based estimators outperform linear ones in these benchmarks (Campadelli et al., 2015), a benchmark has not yet been developed for linguistic data, to our knowledge.

5 Discussion

We have quantified geometric compression in neural language models using the ID of representations, where ID tracks Shannon information-theoretic coding length. This bridges two notions of description length in pre-trained neural LMs by showing they are significantly positively correlated. Our result has also practical implications, suggesting that ID and perplexity predict how easy it is to finetune a model to a task (similarly to what observed in the context of zero-shot prompting by Gonen et al., 2022). More speculatively, the relation between ID and task adaptation may inform future modeling work that actively encourages data compression at training time, to indirectly inject fast-adaptation capabilities into a model.

ID estimators are not equal: we focus on NN-based methods because they explain useful properties of the data and ease-of-finetuning. Our work is a first attempt to evaluate a wide range of ID estimators on natural language representations, and reveals the need for a further principled study of ID estimation of linguistic data.

That nonlinear ID estimators predict information-theoretic compression and ease-of-adaptation over linear ones highlights a need to go beyond PCA in analyzing compression of specific linguistic phenomena. Our experiments on wikitext and variants also demonstrate a need for further experiments on, e.g., idiomaticity, or specific linguistic constructions (cf. Hernandez and Andreas, 2021 for analysis using PCA).

While our work investigates the relationship between ease-of-adaptation and *zero-shot* compression, a logical next step is to investigate how finetuning dynamically affects data compression under the model. We hypothesize that the result may depend on whether the dataset used for finetuning is memorized by the model during training.

Finally, while LMs are trained to reproduce the distribution of human language, it is yet unclear whether analyzing the linguistic representations of the former allows us to make statements about the dimensionality of the latter. Then, an open question remains: what is the "true" dimensionality of natural language, and to what extent do LMs recover it?

Limitations

- While we confirmed that modern LMs do compress language data, and that this compression is correlated with ease-of-learning, we only provided a limited characterization of the relation between LM compression and linguistic properties of the input, such as lexical information and syntactic structure.
- Due to both access restriction and computational limitations, we cannot replicate our investigations on huge language models such as ChatGPT.
- A related question is to what extent the correlation we report between compression and ease of learning would hold (or even how it could be meaningfully formulated) in the context of prompt-based zero-shot task adaptation as afforded by huge LMs.
- More generally, it remains to be explored how a number of modeling choices, such as non-causal predictive objectives or instruction tuning, would affect our generalizations.

Ethics Statement

This paper does not introduce new models or datasets, and it presents an abstract analysis of language model data compression that, we think, should not raise ethical concerns. We believe on the other hand that our focus on improving the understanding of how language models process information can be generally beneficial, in an AI landscape in which powerful language models are deployed with little understanding of the mechanics by which they work, and, consequently, little ability to control their behavior.

Acknowledgements

We thank Alessandro Laio for generous guidance on intrinsic dimensionality estimation. Jacob Andreas provided very helpful feedback on the project. We also thank the members of the UPF COLT lab, especially Gemma Boleda, Roberto Dessì and Lucas Weber for early feedback, the members of the Barcelona Apple Machine Learning Research group and the participants in the EviL seminar for helpful feedback and suggestions. Our work was funded by the European Research Council (ERC) under the European Union's Horizon 2020 research and innovation programme (grant agreement No. 101019291). This paper reflects the authors' view only, and the ERC is not responsible for any use that may be made of the information it contains.

References

Armen Aghajanyan, Sonal Gupta, and Luke Zettlemoyer. 2021. Intrinsic dimensionality explains the effectiveness of language model fine-tuning. In *Proceedings of the 59th Annual Meeting of the Association for Computational Linguistics and the 11th International Joint Conference on Natural Language Processing (Volume 1: Long Papers)*, pages 7319–7328, Online. Association for Computational Linguistics.

Luca Albergante, Jonathan Bac, and Andrei Zinovyev. 2019. Estimating the effective dimension of large biological datasets using fisher separability analysis. In *2019 International Joint Conference on Neural Networks (IJCNN)*, page 1–8.

Laurent Amsaleg, Oussama Chelly, Teddy Furon, Stéphane Girard, Michael E. Houle, Ken-ichi Kawarabayashi, and Michael Nett. 2018. Extreme-value-theoretic estimation of local intrinsic dimensionality. *Data Mining and Knowledge Discovery*, 32(6):1768–1805.

Laurent Amsaleg, Oussama Chelly, Michael E. Houle, Ken-ichi Kawarabayashi, Miloš Radovanović, and Weeris Treeratanajaru. 2019. *Intrinsic Dimensionality Estimation within Tight Localities*, Proceedings, page 181–189. Society for Industrial and Applied Mathematics.

Alessio Ansuini, Alessandro Laio, Jakob H Macke, and Davide Zoccolan. 2019. Intrinsic dimension of data representations in deep neural networks. In *Advances in Neural Information Processing Systems*, volume 32. Curran Associates, Inc.

Sanjeev Arora, Rong Ge, Behnam Neyshabur, and Yi Zhang. 2018. Stronger generalization bounds for deep nets via a compression approach. In *Proceedings of the 35th International Conference on Machine Learning*, volume 80 of *Proceedings of Machine Learning Research*, pages 254–263. PMLR.

Jonathan Bac. 2020. Intrinsic dimension estimation in python — scikit-dimension 0.3.2 documentation.

Dzmitry Bahdanau, Kyunghyun Cho, and Yoshua Bengio. 2015. Neural machine translation by jointly learning to align and translate. In *3rd International Conference on Learning Representations, ICLR 2015, San Diego, CA, USA, May 7-9, 2015, Conference Track Proceedings*.

Francesco Barbieri, Jose Camacho-Collados, Luis Espinosa-Anke, and Leonardo Neves. 2020. TweetEval:Unified Benchmark and Comparative Evaluation for Tweet Classification. In *Proceedings of Findings of EMNLP*.

Stas Bekman. 2022. Openwebtext-10k dataset.

Christopher M. Bishop. 2007. *Pattern Recognition and Machine Learning (Information Science and Statistics)*, 1 edition. Springer.

Léonard Blier and Yann Ollivier. 2018. The description length of deep learning models. In *Advances in Neural Information Processing Systems*, volume 31. Curran Associates, Inc.

Tom Brown, Benjamin Mann, Nick Ryder, Melanie Subbiah, Jared D Kaplan, Prafulla Dhariwal, Arvind Neelakantan, Pranav Shyam, Girish Sastry, Amanda Askell, Sandhini Agarwal, Ariel Herbert-Voss, Gretchen Krueger, Tom Henighan, Rewon Child, Aditya Ramesh, Daniel Ziegler, Jeffrey Wu, Clemens Winter, Chris Hesse, Mark Chen, Eric Sigler, Mateusz Litwin, Scott Gray, Benjamin Chess, Jack Clark, Christopher Berner, Sam McCandlish, Alec Radford, Ilya Sutskever, and Dario Amodei. 2020. Language models are few-shot learners. In *Advances in Neural Information Processing Systems*, volume 33, pages 1877–1901. Curran Associates, Inc.

Xingyu Cai, Jiaji Huang, Yuchen Bian, and Kenneth Church. 2021. Isotropy in the contextual embedding space: Clusters and manifolds. In *International Conference on Learning Representations*.

P. Campadelli, E. Casiraghi, C. Ceruti, and A. Rozza. 2015. Intrinsic dimension estimation: Relevant techniques and a benchmark framework. *Mathematical Problems in Engineering*, 2015:e759567.

Kevin M. Carter, Raviv Raich, and Alfred O. Hero III. 2010. On local intrinsic dimension estimation and its applications. *IEEE Transactions on Signal Processing*, 58(2):650–663.

Claudio Ceruti, Simone Bassis, Alessandro Rozza, Gabriele Lombardi, Elena Casiraghi, and Paola Campadelli. 2014. Danco: An intrinsic dimensionality estimator exploiting angle and norm concentration. *Pattern Recognition*, 47(8):2569–2581.

Ivan Chelombiev, Conor Houghton, and Cian O'Donnell. 2019. Adaptive estimators show information compression in deep neural networks. In *International Conference on Learning Representations*.

Noam Chomsky. 1986. *Knowledge of Language: Its Nature, Origin, and Use*. Praeger, Wesport, CT.

Aakanksha Chowdhery, Sharan Narang, Jacob Devlin, Maarten Bosma, Gaurav Mishra, Adam Roberts, Paul Barham, Hyung Won Chung, Charles Sutton, Sebastian Gehrmann, Parker Schuh, Kensen Shi, Sasha Tsvyashchenko, Joshua Maynez, Abhishek Rao, Parker Barnes, Yi Tay, Noam Shazeer, Vinodkumar Prabhakaran, Emily Reif, Nan Du, Ben Hutchinson, Reiner Pope, James Bradbury, Jacob Austin, Michael Isard, Guy Gur-Ari, Pengcheng Yin, Toju Duke, Anselm Levskaya, Sanjay Ghemawat, Sunipa Dev, Henryk Michalewski, Xavier Garcia, Vedant Misra, Kevin Robinson, Liam Fedus, Denny Zhou, Daphne Ippolito, David Luan, Hyeontaek Lim, Barret Zoph, Alexander Spiridonov, Ryan Sepassi, David Dohan, Shivani Agrawal, Mark Omernick, Andrew M. Dai, Thanumalayan Sankaranarayana Pillai, Marie Pellat, Aitor Lewkowycz, Erica Moreira, Rewon Child, Oleksandr Polozov, Katherine Lee, Zongwei Zhou, Xuezhi Wang, Brennan Saeta, Mark Diaz, Orhan Firat, Michele Catasta, Jason Wei, Kathy Meier-Hellstern, Douglas Eck, Jeff Dean, Slav Petrov, and Noah Fiedel. 2022. Palm: Scaling language modeling with pathways. (arXiv:2204.02311). ArXiv:2204.02311 [cs].

Uri Cohen, SueYeon Chung, Daniel D. Lee, and Haim Sompolinsky. 2020. Separability and geometry of object manifolds in deep neural networks. *Nature Communications*, 11(1):746.

Grégoire Delétang, Anian Ruoss, Paul-Ambroise Duquenne, Elliot Catt, Tim Genewein, Christopher Mattern, Jordi Grau-Moya, Li Kevin Wenliang, Matthew Aitchison, Laurent Orseau, Marcus Hutter, and Joel Veness. 2023. Language modeling is compression.

Francesco Denti, Diego Doimo, Alessandro Laio, and Antonietta Mira. 2022. The generalized ratios intrinsic dimension estimator. *Scientific Reports*, 12(11):20005.

Vittorio Erba, Marco Gherardi, and Pietro Rotondo. 2019. Intrinsic dimension estimation for locally undersampled data. *Scientific Reports*, 9(1):17133.

Elena Facco, Maria d'Errico, Alex Rodriguez, and Alessandro Laio. 2017. Estimating the intrinsic dimension of datasets by a minimal neighborhood information. *Scientific Reports*, 7(1):12140. ArXiv:1803.06992 [cs, stat].

Amir massoud Farahmand, Csaba Szepesvári, and Jean-Yves Audibert. 2007. Manifold-adaptive dimension estimation. In *Proceedings of the 24th international conference on Machine learning*, page 265–272, Corvalis Oregon USA. ACM.

K. Fukunaga and D.R. Olsen. 1971. An algorithm for finding intrinsic dimensionality of data. *IEEE Transactions on Computers*, C-20(2):176–183.

Leo Gao, Stella Biderman, Sid Black, Laurence Golding, Travis Hoppe, Charles Foster, Jason Phang, Horace He, Anish Thite, Noa Nabeshima, et al. 2020. The Pile: An 800GB dataset of diverse text for language modeling. *arXiv preprint arXiv:2101.00027*.

Bernhard C. Geiger. 2022. On information plane analyses of neural network classifiers – a review. *IEEE Transactions on Neural Networks and Learning Systems*, 33(12):7039–7051. ArXiv:2003.09671 [cs, math, stat].

Aaron Gokaslan, Vanya Cohen, Ellie Pavlick, and Stefanie Tellex. 2019. Openwebtext corpus. `http://Skylion007.github.io/OpenWebTextCorpus`.

Ziv Goldfeld, Ewout Van Den Berg, Kristjan Greenewald, Igor Melnyk, Nam Nguyen, Brian Kingsbury, and Yury Polyanskiy. 2019. Estimating information flow in deep neural networks. In *Proceedings of the 36th International Conference on Machine Learning*, volume 97 of *Proceedings of Machine Learning Research*, pages 2299–2308. PMLR.

Hila Gonen, Srini Iyer, Terra Blevins, Noah Smith, and Luke Zettlemoyer. 2022. Demystifying prompts in language models via perplexity estimation. `https://arxiv.org/abs/2212.04037`.

Ian Goodfellow, Yoshua Bengio, and Aaron Courville. 2016. *Deep Learning*. MIT Press. `http://www.deeplearningbook.org`.

Peter Grassberger and Itamar Procaccia. 1983. Measuring the strangeness of strange attractors.

Gloria Haro, Gregory Randall, and Guillermo Sapiro. 2008. Translated poisson mixture model for stratification learning. *International Journal of Computer Vision*, 80(3):358–374.

Karl Moritz Hermann, Tomás Kociský, Edward Grefenstette, Lasse Espeholt, Will Kay, Mustafa Suleyman, and Phil Blunsom. 2015. Teaching machines to read and comprehend. In *NIPS*, pages 1693–1701.

Evan Hernandez and Jacob Andreas. 2021. The low-dimensional linear geometry of contextualized word representations. In *Proceedings of the 25th Conference on Computational Natural Language Learning*, pages 82–93, Online. Association for Computational Linguistics.

Edward J Hu, yelong shen, Phillip Wallis, Zeyuan Allen-Zhu, Yuanzhi Li, Shean Wang, Lu Wang, and Weizhu Chen. 2022. LoRA: Low-rank adaptation of large language models. In *International Conference on Learning Representations*.

Srinivasan Iyer, Ioannis Konstas, Alvin Cheung, and Luke Zettlemoyer. 2018. Mapping language to code in programmatic context. In *Proceedings of the 2018 Conference on Empirical Methods in Natural Language Processing*, page 1643–1652, Brussels, Belgium. Association for Computational Linguistics.

Kerstin Johnsson, Charlotte Soneson, and Magnus Fontes. 2015. Low bias local intrinsic dimension estimation from expected simplex skewness. *IEEE transactions on pattern analysis and machine intelligence*, 37(1):196–202.

Ian Jolliffe. 1986. *Principal Component Analysis*. Springer.

Elizaveta Levina and Peter Bickel. 2004. Maximum likelihood estimation of intrinsic dimension. In *Advances in Neural Information Processing Systems*, volume 17. MIT Press.

Chunyuan Li, Heerad Farkhoor, Rosanne Liu, and Jason Yosinski. 2018. Measuring the intrinsic dimension of objective landscapes. In *International Conference on Learning Representations*.

Percy Liang, Rishi Bommasani, Tony Lee, Dimitris Tsipras, Dilara Soylu, Michihiro Yasunaga, Yian Zhang, Deepak Narayanan, Yuhuai Wu, Ananya Kumar, Benjamin Newman, Binhang Yuan, Bobby Yan, Ce Zhang, Christian Cosgrove, Christopher D. Manning, Christopher Ré, Diana Acosta-Navas, Drew A. Hudson, Eric Zelikman, Esin Durmus, Faisal Ladhak, Frieda Rong, Hongyu Ren, Huaxiu Yao, Jue Wang, Keshav Santhanam, Laurel Orr, Lucia Zheng, Mert Yuksekgonul, Mirac Suzgun, Nathan Kim, Neel Guha, Niladri Chatterji, Omar Khattab, Peter Henderson, Qian Huang, Ryan Chi, Sang Michael Xie, Shibani Santurkar, Surya Ganguli, Tatsunori Hashimoto, Thomas Icard, Tianyi Zhang, Vishrav Chaudhary, William Wang, Xuechen Li, Yifan Mai, Yuhui Zhang, and Yuta Koreeda. 2022. Holistic evaluation of language models.

Ilya Loshchilov and Frank Hutter. 2019. Decoupled weight decay regularization. In *International Conference on Learning Representations*.

Andrew L. Maas, Raymond E. Daly, Peter T. Pham, Dan Huang, Andrew Y. Ng, and Christopher Potts. 2011. Learning word vectors for sentiment analysis. In *Proceedings of the 49th Annual Meeting of the Association for Computational Linguistics: Human Language Technologies*, pages 142–150, Portland, Oregon, USA. Association for Computational Linguistics.

Jonathan Mamou, Hang Le, Miguel Del Rio, Cory Stephenson, Hanlin Tang, Yoon Kim, and Sueyeon Chung. 2020. Emergence of separable manifolds in deep language representations. In *Proceedings of the 37th International Conference on Machine Learning*, page 6713–6723. PMLR.

Mitchell P. Marcus, Beatrice Santorini, and Mary Ann Marcinkiewicz. 1993. Building a large annotated corpus of English: The Penn Treebank. *Computational Linguistics*, 19(2):313–330.

Stephen Merity, Caiming Xiong, James Bradbury, and Richard Socher. 2017. Pointer sentinel mixture models. In *International Conference on Learning Representations*.

Francis Mollica and Steven Piantadosi. 2019. Humans store about 1.5 megabytes of information during language acquisition. *Royal Society Open Science*, 6(3):181393.

Neel Nanda. 2022. Pile-10k dataset.

Morteza Noshad, Yu Zeng, and Alfred O. Hero. 2019. Scalable mutual information estimation using dependence graphs. In *ICASSP 2019 - 2019 IEEE International Conference on Acoustics, Speech and Signal Processing (ICASSP)*, page 2962–2966.

OpenAI. 2023. Gpt-4 technical report. (arXiv:2303.08774). ArXiv:2303.08774 [cs].

Ethan Perez, Douwe Kiela, and Kyunghyun Cho. 2021. Rissanen data analysis: Examining dataset characteristics via description length. In *Proceedings of the 38th International Conference on Machine Learning*, page 8500–8513. PMLR.

Phil Pope, Chen Zhu, Ahmed Abdelkader, Micah Goldblum, and Tom Goldstein. 2021. The intrinsic dimension of images and its impact on learning. In *International Conference on Learning Representations*.

Alec Radford and Karthik Narasimhan. 2018. Improving language understanding by generative pretraining.

Stefano Recanatesi, Matthew Farrell, Madhu Advani, Timothy Moore, Guillaume Lajoie, and Eric Shea-Brown. 2019. Dimensionality compression and expansion in deep neural networks. ArXiv:1906.00443 [cs, stat].

Anna Rogers, Olga Kovaleva, and Anna Rumshisky. 2020. A primer in BERTology: What we know about how BERT works. *Transactions of the Association for Computational Linguistics*, 8:842–866.

A. Rozza, G. Lombardi, C. Ceruti, E. Casiraghi, and P. Campadelli. 2012. Novel high intrinsic dimensionality estimators. *Machine Learning*, 89(1):37–65.

Andrew Michael Saxe, Yamini Bansal, Joel Dapello, Madhu Advani, Artemy Kolchinsky, Brendan Daniel Tracey, and David Daniel Cox. 2018. On the information bottleneck theory of deep learning. In *International Conference on Learning Representations*.

C E Shannon. 1948. A mathematical theory of communication.

Ravid Shwartz-Ziv and Naftali Tishby. 2017. Opening the black box of deep neural networks via information.

Antoine Simoulin and Benoit Crabbé. 2021. Un modèle Transformer Génératif Pré-entrainé pour le ______ français. In *Traitement Automatique des Langues Naturelles*, pages 246–255, Lille, France. ATALA.

Ahmed Soliman. 2022. Codexglue-concode dataset.

Aarohi Srivastava, Abhinav Rastogi, Abhishek Rao, Abu Awal Md Shoeb, Abubakar Abid, Adam Fisch, Adam R. Brown, Adam Santoro, Aditya Gupta, Adrià Garriga-Alonso, Agnieszka Kluska, Aitor Lewkowycz, Akshat Agarwal, Alethea Power, Alex Ray, Alex Warstadt, Alexander W. Kocurek, Ali Safaya, Ali Tazarv, Alice Xiang, Alicia Parrish, Allen Nie, Aman Hussain, Amanda Askell, Amanda Dsouza, Ambrose Slone, Ameet Rahane, Anantharaman S. Iyer, Anders Andreassen, Andrea Madotto, Andrea Santilli, Andreas Stuhlmüller, Andrew Dai, Andrew La, Andrew Lampinen, Andy Zou, Angela Jiang, Angelica Chen, Anh Vuong, Animesh Gupta, Anna Gottardi, Antonio Norelli, Anu Venkatesh, Arash Gholamidavoodi, Arfa Tabassum, Arul Menezes, Arun Kirubarajan, Asher Mullokandov, Ashish Sabharwal, Austin Herrick, Avia Efrat, Aykut Erdem, Ayla Karakaş, B. Ryan Roberts, Bao Sheng Loe, Barret Zoph, Bartłomiej Bojanowski, Batuhan Özyurt, Behnam Hedayatnia, Behnam Neyshabur, Benjamin Inden, Benno Stein, Berk Ekmekci, Bill Yuchen Lin, Blake Howald, Cameron Diao, Cameron Dour, Catherine Stinson, Cedrick Argueta, César Ferri Ramírez, Chandan Singh, Charles Rathkopf, Chenlin Meng, Chitta Baral, Chiyu Wu, Chris Callison-Burch, Chris Waites, Christian Voigt, Christopher D. Manning, Christopher Potts, Cindy Ramirez, Clara E. Rivera, Clemencia Siro, Colin Raffel, Courtney Ashcraft, Cristina Garbacea, Damien Sileo, Dan Garrette, Dan Hendrycks, Dan Kilman, Dan Roth, Daniel Freeman, Daniel Khashabi, Daniel Levy, Daniel Moseguí González, Danielle Perszyk, Danny Hernandez, Danqi Chen, Daphne Ippolito, Dar Gilboa, David Dohan, David Drakard, David Jurgens, Debajyoti Datta, Deep Ganguli, Denis Emelin, Denis Kleyko, Deniz Yuret, Derek Chen, Derek Tam, Dieuwke Hupkes, Diganta Misra, Dilyar Buzan, Dimitri Coelho Mollo, Diyi Yang, Dong-Ho Lee, Ekaterina Shutova, Ekin Dogus Cubuk, Elad Segal, Eleanor Hagerman, Elizabeth Barnes, Elizabeth Donoway, Ellie Pavlick, Emanuele Rodola, Emma Lam, Eric Chu, Eric Tang, Erkut Erdem, Ernie Chang, Ethan A. Chi, Ethan Dyer, Ethan Jerzak, Ethan Kim, Eunice Engefu Manyasi, Evgenii Zheltonozhskii, Fanyue Xia, Fatemeh Siar, Fernando Martínez-Plumed, Francesca Happé, Francois Chollet, Frieda Rong, Gaurav Mishra, Genta Indra Winata, Gerard de Melo, Germán Kruszewski, Giambattista Parascandolo, Giorgio Mariani, Gloria Wang, Gonzalo Jaimovitch-López, Gregor Betz, Guy Gur-Ari, Hana Galijasevic, Hannah Kim, Hannah Rashkin, Hannaneh Hajishirzi, Harsh Mehta, Hayden Bogar, Henry Shevlin, Hinrich Schütze, Hiromu Yakura, Hongming Zhang, Hugh Mee Wong, Ian Ng, Isaac Noble, Jaap Jumelet, Jack Geissinger, Jackson Kernion, Jacob Hilton, Jaehoon Lee, Jaime Fernández Fisac, James B. Simon, James Koppel, James Zheng, James Zou, Jan Kocoń, Jana Thompson, Jared Kaplan, Jarema Radom, Jascha Sohl-Dickstein, Jason Phang, Jason Wei, Jason Yosinski, Jekaterina Novikova, Jelle Bosscher, Jennifer Marsh, Jeremy Kim, Jeroen Taal, Jesse Engel, Jesujoba Alabi, Jiacheng Xu, Jiaming Song, Jillian Tang, Joan Waweru, John Burden, John Miller, John U. Balis, Jonathan Berant, Jörg Frohberg, Jos Rozen, Jose Hernandez-Orallo, Joseph Boudeman, Joseph Jones, Joshua B. Tenenbaum, Joshua S. Rule, Joyce Chua, Kamil Kanclerz, Karen Livescu, Karl Krauth, Karthik Gopalakrishnan, Katerina Ignatyeva, Katja Markert, Kaustubh D. Dhole, Kevin Gimpel, Kevin Omondi, Kory Mathewson, Kristen Chiafullo, Ksenia Shkaruta, Kumar Shridhar, Kyle McDonell, Kyle Richardson, Laria Reynolds, Leo Gao, Li Zhang, Liam Dugan, Lianhui Qin, Lidia Contreras-Ochando, Louis-Philippe Morency, Luca Moschella, Lucas Lam, Lucy Noble, Ludwig Schmidt, Luheng

He, Luis Oliveros Colón, Luke Metz, Lütfi Kerem Şenel, Maarten Bosma, Maarten Sap, Maartje ter Hoeve, Maheen Farooqi, Manaal Faruqui, Mantas Mazeika, Marco Baturan, Marco Marelli, Marco Maru, Maria Jose Ramírez Quintana, Marie Tolkiehn, Mario Giulianelli, Martha Lewis, Martin Potthast, Matthew L. Leavitt, Matthias Hagen, Mátyás Schubert, Medina Orduna Baitemirova, Melody Arnaud, Melvin McElrath, Michael A. Yee, Michael Cohen, Michael Gu, Michael Ivanitskiy, Michael Starritt, Michael Strube, Michał Swędrowski, Michele Bevilacqua, Michihiro Yasunaga, Mihir Kale, Mike Cain, Mimee Xu, Mirac Suzgun, Mo Tiwari, Mohit Bansal, Moin Aminnaseri, Mor Geva, Mozhdeh Gheini, Mukund Varma T, Nanyun Peng, Nathan Chi, Nayeon Lee, Neta Gur-Ari Krakover, Nicholas Cameron, Nicholas Roberts, Nick Doiron, Nikita Nangia, Niklas Deckers, Niklas Muennighoff, Nitish Shirish Keskar, Niveditha S. Iyer, Noah Constant, Noah Fiedel, Nuan Wen, Oliver Zhang, Omar Agha, Omar Elbaghdadi, Omer Levy, Owain Evans, Pablo Antonio Moreno Casares, Parth Doshi, Pascale Fung, Paul Pu Liang, Paul Vicol, Pegah Alipoormolabashi, Peiyuan Liao, Percy Liang, Peter Chang, Peter Eckersley, Phu Mon Htut, Pinyu Hwang, Piotr Miłkowski, Piyush Patil, Pouya Pezeshkpour, Priti Oli, Qiaozhu Mei, Qing Lyu, Qinlang Chen, Rabin Banjade, Rachel Etta Rudolph, Raefer Gabriel, Rahel Habacker, Ramón Risco Delgado, Raphaël Millière, Rhythm Garg, Richard Barnes, Rif A. Saurous, Riku Arakawa, Robbe Raymaekers, Robert Frank, Rohan Sikand, Roman Novak, Roman Sitelew, Ronan LeBras, Rosanne Liu, Rowan Jacobs, Rui Zhang, Ruslan Salakhutdinov, Ryan Chi, Ryan Lee, Ryan Stovall, Ryan Teehan, Rylan Yang, Sahib Singh, Saif M. Mohammad, Sajant Anand, Sam Dillavou, Sam Shleifer, Sam Wiseman, Samuel Gruetter, Samuel R. Bowman, Samuel S. Schoenholz, Sanghyun Han, Sanjeev Kwatra, Sarah A. Rous, Sarik Ghazarian, Sayan Ghosh, Sean Casey, Sebastian Bischoff, Sebastian Gehrmann, Sebastian Schuster, Sepideh Sadeghi, Shadi Hamdan, Sharon Zhou, Shashank Srivastava, Sherry Shi, Shikhar Singh, Shima Asaadi, Shixiang Shane Gu, Shubh Pachchigar, Shubham Toshniwal, Shyam Upadhyay, Shyamolima, Debnath, Siamak Shakeri, Simon Thormeyer, Simone Melzi, Siva Reddy, Sneha Priscilla Makini, Soo-Hwan Lee, Spencer Torene, Sriharsha Hatwar, Stanislas Dehaene, Stefan Divic, Stefano Ermon, Stella Biderman, Stephanie Lin, Stephen Prasad, Steven T. Piantadosi, Stuart M. Shieber, Summer Misherghi, Svetlana Kiritchenko, Swaroop Mishra, Tal Linzen, Tal Schuster, Tao Li, Tao Yu, Tariq Ali, Tatsu Hashimoto, Te-Lin Wu, Théo Desbordes, Theodore Rothschild, Thomas Phan, Tianle Wang, Tiberius Nkinyili, Timo Schick, Timofei Kornev, Timothy Telleen-Lawton, Titus Tunduny, Tobias Gerstenberg, Trenton Chang, Trishala Neeraj, Tushar Khot, Tyler Shultz, Uri Shaham, Vedant Misra, Vera Demberg, Victoria Nyamai, Vikas Raunak, Vinay Ramasesh, Vinay Uday Prabhu, Vishakh Padmakumar, Vivek Srikumar, William Fedus, William Saunders, William Zhang, Wout Vossen, Xiang Ren, Xiaoyu Tong, Xinran Zhao, Xinyi Wu, Xudong Shen, Yadollah Yaghoobzadeh, Yair Lakretz, Yangqiu Song, Yasaman Bahri, Yejin Choi, Yichi Yang, Yiding Hao, Yifu Chen, Yonatan Belinkov, Yu Hou, Yufang Hou, Yuntao Bai, Zachary Seid, Zhuoye Zhao, Zijian Wang, Zijie J. Wang, Zirui Wang, and Ziyi Wu. 2022. Beyond the imitation game: Quantifying and extrapolating the capabilities of language models. (arXiv:2206.04615). ArXiv:2206.04615 [cs, stat].

Naftali Tishby and Noga Zaslavsky. 2015. Deep learning and the information bottleneck principle. In *2015 IEEE Information Theory Workshop (ITW)*, page 1–5.

Hugo Touvron, Louis Martin, Kevin Stone, Peter Albert, Amjad Almahairi, Yasmine Babaei, Nikolay Bashlykov, Soumya Batra, Prajjwal Bhargava, Shruti Bhosale, Dan Bikel, Lukas Blecher, Cristian Canton Ferrer, Moya Chen, Guillem Cucurull, David Esiobu, Jude Fernandes, Jeremy Fu, Wenyin Fu, Brian Fuller, Cynthia Gao, Vedanuj Goswami, Naman Goyal, Anthony Hartshorn, Saghar Hosseini, Rui Hou, Hakan Inan, Marcin Kardas, Viktor Kerkez, Madian Khabsa, Isabel Kloumann, Artem Korenev, Punit Singh Koura, Marie-Anne Lachaux, Thibaut Lavril, Jenya Lee, Diana Liskovich, Yinghai Lu, Yuning Mao, Xavier Martinet, Todor Mihaylov, Pushkar Mishra, Igor Molybog, Yixin Nie, Andrew Poulton, Jeremy Reizenstein, Rashi Rungta, Kalyan Saladi, Alan Schelten, Ruan Silva, Eric Michael Smith, Ranjan Subramanian, Xiaoqing Ellen Tan, Binh Tang, Ross Taylor, Adina Williams, Jian Xiang Kuan, Puxin Xu, Zheng Yan, Iliyan Zarov, Yuchen Zhang, Angela Fan, Melanie Kambadur, Sharan Narang, Aurelien Rodriguez, Robert Stojnic, Sergey Edunov, and Thomas Scialom. 2023. Llama 2: Open foundation and fine-tuned chat models. (arXiv:2307.09288). ArXiv:2307.09288 [cs].

Lucrezia Valeriani, Diego Doimo, Francesca Cuturello, Alessandro Laio, Alessio Ansuini, and Alberto Cazzaniga. 2023. The geometry of hidden representations of large transformer models. (arXiv:2302.00294). ArXiv:2302.00294 [cs, stat].

Ashish Vaswani, Noam Shazeer, Niki Parmar, Jakob Uszkoreit, Llion Jones, Aidan N Gomez, Łukasz Kaiser, and Illia Polosukhin. 2017. Attention is all you need. In *Advances in Neural Information Processing Systems*, volume 30. Curran Associates, Inc.

Elena Voita and Ivan Titov. 2020. Information-theoretic probing with minimum description length. In *Proceedings of the 2020 Conference on Empirical Methods in Natural Language Processing (EMNLP)*, page 183–196, Online. Association for Computational Linguistics.

Alex Wang, Yada Pruksachatkun, Nikita Nangia, Amanpreet Singh, Julian Michael, Felix Hill, Omer Levy, and Samuel Bowman. 2019a. Superglue: A stickier benchmark for general-purpose language understanding systems. In *Advances in Neural Information Processing Systems*, volume 32. Curran Associates, Inc.

Alex Wang, Amanpreet Singh, Julian Michael, Felix Hill, Omer Levy, and Samuel Bowman. 2019b. GLUE: A multi-task benchmark and analysis platform for natural language understanding. In *Proceedings of ICLR*, New Orleans, LA. Published online: https://openreview.net/group?id=ICLR.cc/2019/conference.

Jason Wei, Yi Tay, Rishi Bommasani, Colin Raffel, Barret Zoph, Sebastian Borgeaud, Dani Yogatama, Maarten Bosma, Denny Zhou, Donald Metzler, Ed H. Chi, Tatsunori Hashimoto, Oriol Vinyals, Percy Liang, Jeff Dean, and William Fedus. 2022. Emergent abilities of large language models. *Transactions on Machine Learning Research*.

Susan Zhang, Stephen Roller, Naman Goyal, Mikel Artetxe, Moya Chen, Shuohui Chen, Christopher Dewan, Mona Diab, Xian Li, Xi Victoria Lin, Todor Mihaylov, Myle Ott, Sam Shleifer, Kurt Shuster, Daniel Simig, Punit Singh Koura, Anjali Sridhar, Tianlu Wang, and Luke Zettlemoyer. 2022. Opt: Open pre-trained transformer language models. (arXiv:2205.01068). ArXiv:2205.01068 [cs].

Yu Zhang, Peter Tiňo, Aleš Leonardis, and Ke Tang. 2021. A survey on neural network interpretability. *IEEE Transactions on Emerging Topics in Computational Intelligence*, 5(5):726–742.

Zhong Zhang, Bang Liu, and Junming Shao. 2023. Fine-tuning happens in tiny subspaces: Exploring intrinsic task-specific subspaces of pre-trained language models. In *Proceedings of the 61st Annual Meeting of the Association for Computational Linguistics (Volume 1: Long Papers)*, pages 1701–1713, Toronto, Canada. Association for Computational Linguistics.

Y. Zhu, R. Kiros, R. Zemel, R. Salakhutdinov, R. Urtasun, A. Torralba, and S. Fidler. 2015. Aligning books and movies: Towards story-like visual explanations by watching movies and reading books. In *2015 IEEE International Conference on Computer Vision (ICCV)*, pages 19–27, Los Alamitos, CA, USA. IEEE Computer Society.

A ID Estimation

In this appendix, we detail the tested ID estimation methods (appendix A.1) and validate their convergence on a sample of $50,000$ datapoints of the `bookcorpus` dataset in appendix A.2.

A.1 ID Estimator Details

For each ID estimator tested, we provide a brief description as well as the hyperparameters used (which we will denote k) in relation to the `skdim` package. As ID estimation theory is not our focus, we refer the reader to Campadelli et al., 2015 for a comprehensive review of methods.

Note that ID estimators can be classified as *global* or *local*. Global ID estimation assumes the entire dataset lies on a single geometric object, and estimates its dimensionality from the entire dataset at once. In contrast, local ID estimation computes point-wise ID of data neighborhoods, then aggregates the per-neighborhood estimates to arrive at a global estimate. This aggregation of local estimates can correct for negative biases of global ID estimators in high d, where this bias is symptomatic of concentration of measure in high dimensions (Carter et al., 2010). While Mamou et al., 2020 show that linguistic representations lie on separable manifolds, we assumed for simplicity that our data lie on one geometric object and use either global or local methods to estimate its ID, leaving per-manifold ID estimation to future work.

Estimator	Method	Global/Local
PCA	Projective	Global
FisherS	Fine-grained clustering	Global
CorrInt	Fractal	Global
TwoNN	NN-based	Global
KNN	NN-based	Global
MiND ML	NN-based	Global
DANCo	NN-based	Global
TLE	NN-based	Local
MLE	NN-based	Local
MOM	NN-based	Local
MADA	NN-based	Local
ESS	NN-based	Local

Table A.1: Taxonomy of 12 ID estimators tested (3 of which unsuccessfully: KNN, MiND ML, and DANCo), by method and by whether global or local. If local, point-wise ID estimates are computed and mean-aggregated.

A.1.1 Global Estimators

PCA Projective method that assumes a linear manifold. The ID d is the number of principal values $\lambda > \frac{\lambda_{max}}{k}$, where hyperparameter $k = 20$ (Fukunaga and Olsen, 1971).

Fisher Separability (FisherS) Fine-grained clustering estimator that relies on "clumping" phenomena in high dimensions. To estimate d, (1) the data are transformed using PCA (hyperparameter $k = 10$) and projected onto the unit sphere; (2) the proportion of linearly separable datapoints is compared to that of a theoretical equidistribution on a d-sphere (Albergante et al., 2019).

Correlation Dimension (CorrInt) The volume s of a d-dimensional radius-r hypersphere grows as $s \sim r^d$. For two values of r: r_1 and r_2, estimate s by counting the nearest neighbors in a radius-r sphere around each point. Then, fit d (Grassberger and Procaccia, 1983).

We choose r_1 corresponding to hyperparameter $k_1 = 10$ nearest neighbors and r_2 corresponding to hyperparameter $k_2 = 20$ nearest neighbors.

TwoNN A nearest-neighbors (NN)-based estimator that assumes local uniform data density (up to the second neighbor). Regresses $\frac{\log(1-F(\mu))}{\log \mu} = d$, where F is the cumulative density function and $\mu_i := \frac{r_2}{r_1}$ is the 2NNs distance ratio for each $x_i \in X$. Following Facco et al., 2017, we discard hyperparameter $k = 0.1$ fraction of largest μ_i from the regression, a heuristic that improves estimation accuracy.

A.1.2 Local Estimators

ESS For each datapoint, take hyperparameter $k = 10$ nearest neighbors. This neighborhood is assumed to be approximable by a uniform distribution of datapoints on a tangent plane to the manifold. Expected Simplex Skewness, or ESS (called *ESSa* in Johnsson et al., 2015), constructs a simplex with one vertex at the centroid of the local dataset and other vertices at the other datapoints. Then, the expected simplex skewness measure is defined as the volume of the simplex divided by the volume if all edges to the centroid were orthogonal. The ESS is computed over all such local datasets then compared to the theoretical expected value in d-dimensions in order to estimate d.

TLE Tight Local ID Estimation consists of computing a modified Correlation Dimension on small neighborhoods of hyperparameter $k = 20$ neighbors around query datapoints, then fitting d using maximum-likelihood estimation (Amsaleg et al., 2019).

MLE We use the Maximum Likelihood Estimator of Haro et al., 2008, which extends Levina and Bickel, 2004 to handle noise. For simplicity, we assume one underlying data manifold (the method extends to multiple underlying manifolds). Then, MLE models the number of points falling into a small neighborhood around query points by a (Translated) Poisson process. The maximum-likelihood estimator for the Poisson λ parameter is fit given data, from which one can solve for the local ID at that neighborhood. Finally, local IDs are averaged to arrive at the overall estimate.

MOM The Method-of-Moments estimator from Amsaleg et al., 2018 takes as reference the distribution of distances X to a query point q, over hyperparameter $k = 100$ NNs of q. The procedure estimates empirical moments of X and compares them to the theoretical value, which is a function of d, in order to solve for d.

MADA Manifold Adaptive Dimension Estimation (MADA) compares the empirical probability that datapoints fall into a ball around a query datapoint to the theoretical probability, which is a function of d. More precisely,

$$\mathbb{P}(x_i \in B(x, r)) = \eta(x, r) r^d$$

for some function η, where for small-enough r, $\eta(x, r)$ is essentially constant. Then, d is fit over many query points x and x_i in the dataset (Farahmand et al., 2007).

A.2 ID Estimation Convergence Analysis

In section 3.1, we state that ID estimation is performed for datasets X of size $N > 10000$. For large datasets ($N > 50000$), we compute ID on random subsample of $\min(N, 50000)$ data points for efficiency. Here, we verify that ID computed on a sample of size $10000 < N < 50000$ for $\max(D) = 4096$ reasonably converges, the reason being that NN-based ID estimators can be *scale-dependent*. Scale-dependence, or sensitivity to data resolution, of NN-based estimators is well-documented in the literature. Due to concentration of measure in high dimensions, these estimators are sensitive to data density and underestimate ID for $d \gtrsim 10$ (Facco et al., 2017; Ansuini et al., 2019; Ceruti et al., 2014), see Erba et al., 2019 for discussion.

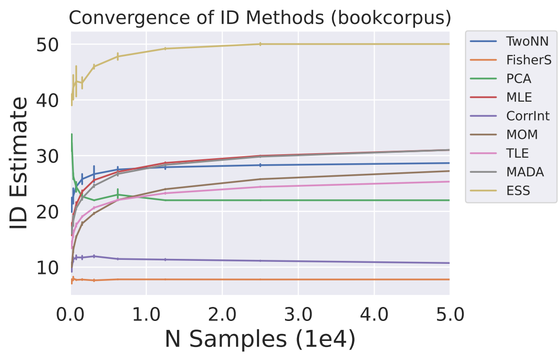

Figure A.1: Convergence of ID estimates for `bookcorpus` on the last layer of OPT-6.7b, from $N' \approx 200$ to $N' = 50000$. Each datapoint is the mean ID estimate, shown with one standard deviation, on a bootstrapped sample of size N', computed over 3 random seeds.

Similar to Ansuini et al., 2019, we justify our choice of 50000 with a convergence analysis of ID estimators on a large, complex dataset, that is, `bookcorpus` ($N = 74004228$), using OPT-6.7b ($D = 4096$), and a one layer representation (the last). Starting at $N' = 50000$, we systematically subsample the representations on a log-scale and show that ID estimates averaged over three random seeds appear to converge for all estimators by $N' \approx 10000$ (see fig. A.1). Convergence of these estimates permits us to reliably include them in our analysis linking ID to PPL and ease-of-adaptation.

Finally, our approach is limited for small datasets, as N needs to grow exponentially in d in order to estimate d (Bishop, 2007). As attested in the literature (Campadelli et al., 2015; Albergante et al., 2019), several ID estimators are empirically more robust to this curse of dimensionality, such as non-NN-based estimators PCA and FisherS, which converge earlier than $N' \approx 10000$. Moreover, note that for the remaining ID estimators, for small $N' \lessapprox 10000$, they are increasing, thus systematically underestimating ID, until starting to converge at around $N' \approx 10000$. Therefore, while $N' = 10000$ is not an end-all be-all cut-off for ID convergence of linguistic data, we employ it as a heuristic for dataset selection.

A.3 Other Estimators Tested

We tested a total of 12 estimators. In addition to the 9 discussed in appendix A.1, we tested three NN-based global estimators, DANCo (Ceruti et al., 2014), MiND ML (Rozza et al., 2012), and kNN (without bootstrapping) (Carter et al., 2010), but encountered difficulty tuning the hyperparameters to produce sensible ID estimates (MiND ML produced $d = 10$ for almost all layers on all datasets; the other estimators produced $d \approx D$). For this reason, we omit them from discussion of the results.

Finally, in future work, it is worth testing the recent FCI estimator of Erba et al., 2019 and the Generalized Ratios ID estimator of Denti et al., 2022, which are more robust to scaling effects by design.

B Dataset Details

In this appendix, we outline how [Super]GLUE data are preprocessed for PPL and ID computation, and describe the remaining corpora in table B.2. All datasets are freely available on HuggingFace at the time of writing.

Preprocessing [Super]GLUE GLUE and SuperGLUE are two linguistic classification benchmarks designed to test language models on tasks such as textual entailment and semantic equivalence (Wang et al., 2019b,a). For example, in Quora Question Pairs (qqp), two questions are given to the model as natural language, and the model is tasked to predict whether they are equivalent. If there are multiple inputs, we treat them as individual data points in the ID / PPL computations and feed them to the model separately as in Wang et al., 2019a, leaving other strategies, such as concatenation with delimiters (Brown et al., 2020), to future work.

C Finetuning Details

We implement full finetuning for OPT-350m and parameter-efficient finetuning using LoRA (Hu et al., 2022) for the other LMs on a standard cross-entropy causal language modeling objective, optimized using AdamW (Loshchilov and Hutter, 2019).

To avoid an expensive hyperparameter search, we set a constant batch size for each model (the largest fitting in memory), with a constant learning rate schedule. Then, the only hyperparameter we vary is the learning rate from 5e-5, 5e-6 to 5e-7. For each learning rate, we average final evaluation PPL after training over three random seeds, and we choose the best learning rate by the lowest final evaluation PPL. All values reported are averaged over 3 random seeds for the best learning rate.

Corpus	Summary
IMDB (Maas et al., 2011)	Movie reviews
Penn Treebank (Marcus et al., 1993)	Text-only version of Penn Treebank (content from 1989 Wall Street Journal)
Bookcorpus (Zhu et al., 2015)	Text from books
Wikitext (Merity et al., 2017)	Cleaned Wikipedia
Wikitext fr (Simoulin and Crabbé, 2021)	Cleaned French Wikipedia
Tweets (Barbieri et al., 2020)	Twitter dataset's sentiment evaluation subset
Pile-10k (Nanda, 2022)	First 10k sequences of The Pile (Gao et al., 2020)
Openwebtext-10k (Bekman, 2022)	10k sequences from Openwebtext (Gokaslan et al., 2019)
CNN Dailymail (Hermann et al., 2015)	News articles from CNN
CONCODE (Soliman, 2022)	Set of Java classes from CONCODE (Iyer et al., 2018)

Table B.2: Description of external non-[Super]GLUE corpora

Hyperparameter	Value
Batch size	8 (opt-350m); 16 (opt-6.7b); 32 (opt-1.3b)
lr	5e-5, 5e-6, 5e-7
max train epochs	15
LoRA rank	8
LoRA α	8
AdamW β_1, β_2	(0.9, 0.999)
AdamW ϵ	1e-6

Table C.3: Hyperparameters used in finetuning, where OPT-350m is fully finetuned and all other models are finetuned using LoRA.

Hyperparameters can be found in table C.3. Code is adapted from HuggingFace implementations and can be found at `https://github.com/`

chengemily1/id_bridging.

D ID over layers

In Section 4, we have presented results focusing on max ID as our aggregate measure across layers. However, the evolution of ID across layers is an interesting problem in itself, and reveals how Transformers sequentially compress (or decompress) linguistic representations (cf. Valeriani et al., 2023 and Ansuini et al., 2019 for equivalent studies on protein sequence and vision models, respectively).

In the large majority of cases, ID is relatively stable across layers, justifying the choice of focusing on an aggregate measure: see representative examples in fig. D.2a. We do, however, also observe small clusters of datasets where the ID profile across layers exhibits different patterns. For example, for a number of datasets (example in fig. D.2b), we observe a first increase in ID in the early layers followed by a later increase at the middle layers, which might suggest kernel-function-like dimensionality expansions before new reductions, along the lines of what was observed by Ansuini et al., 2019. Another interesting pattern pertains to the OPTCorpus, showing a late increase in dimensionality. Intriguingly, this pattern is not disrupted by the ablations, as shown in fig. D.2c. Still, we want to emphasize that in most cases ID profiles are relatively flat: even when they aren't (as in figs. D.2b and D.2c), the fluctuations stay within relatively narrow ranges. We conjecture that residual connections have a stabilizing effect on ID across layers. Notably, however, Valeriani et al., 2023 found that Transformers applied to visual and protein sequence data displayed an early peak in ID that is missing in our linguistic datasets, whose profiles vary in shape. We leave a fuller understanding of the differences to future work.

E Extended Results

Here, we review results on the relationship between geometric compression, information-theoretic compression, and ease-of-adaptation for all model sizes, ID estimators, and aggregations of ID.

Alternative Aggregations of ID In addition to the max ID over layers, which is discussed in the main article, we test the following other aggregations: min, first (ID of positional embeddings), last (ID before next-word prediction), mean, and median, which are "point-aggregates" of ID, and change (last−first) and range (max−min), which summarize the spread of ID, i.e., how data is processed in terms of expansion or reduction over layers.

We find that when one aggregation of ID is correlated to PPL, so are other aggregations. For instance, as the max ID influences the mean ID, they are often both correlated to PPL. For estimators CorrInt, TwoNN, ESS, TLE, and MLE, we notice virtually all aggregations of ID correlating to perplexity in OPT-350m (right column of figs. E.6 and E.7).

ID vs. Perplexity We observe the following about the Spearman correlation between aggregations of ID and dataset perplexity:

- **Correlation strength tends to increase as model size decreases**. This is seen by looking at the leftmost columns of the correlation plots: there are more significant correlations (colored squares) as model size decreases in figs. E.6 and E.7.
- When significant, **min, max, first, last, mean, and median ID are *positively correlated* to PPL** for all model sizes and ID estimators.
- When significant, **change in ID is *negatively* correlated with PPL** for all model sizes and ID estimators. That is, intuitively, if an input is harder for the model to process (larger PPL), it projects its features into higher-dimensional space for next-token prediction, which we interpret to be a kernel-expansion-like operation à la Ansuini et al., 2019.
- When significant, **range of ID positively correlates to PPL** for all model sizes and ID estimators. This correlation can be partially explained by those between the min and max ID and PPL.

ID vs. Ease-of-Adaptation We find that several ID aggregates are good predictors of ease-of-adaptation across model size and ID estimator. We observe the following:

- For Correlation Dimension and NN-based ID estimators, when significant, **point estimates of ID (e.g., max, mean) positively correlate to final evaluation PPL and sample complexity**, as evidenced by the orange-colored squares in the bottom-right of plots in figs. E.6 and E.7. This trend breaks down for PCA and FisherS, but appears robust to model size.

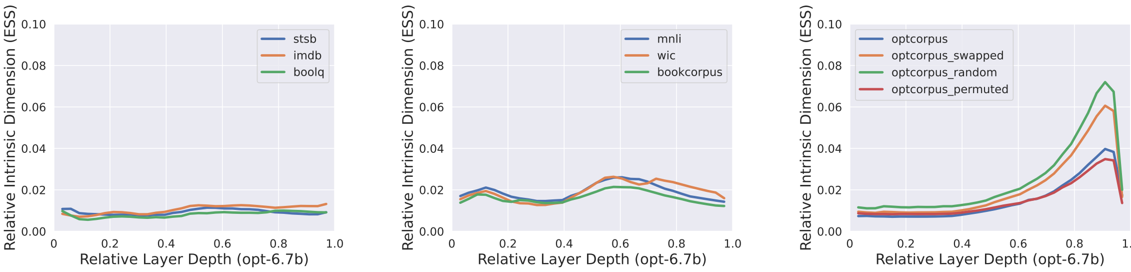

(a) Relatively stable ID (b) Expansions then reductions in ID (c) ID profiles for OPTCorpora

Figure D.2: Representative (relative) ID profiles, computed with ESS, of dataset representations against layer depth for OPT-6.7b, qualitatively grouped into three categories: (a) “flat" (the most common case), (b) “hilly", and (c) gradual increase then sudden decrease, corresponding to OPTCorpora. ID profiles are calculated on $\min(N, 50000)$ sequences for each dataset shown, where N is the number of sequences in the dataset.

- **Results on ID spread (change and range) are inconclusive**, giving sometimes negative and sometimes positive correlations depending on the estimator and model size.

ID vs. Shallow Linguistic Descriptors The relationship between ID and shallow linguistic descriptors like vocab size, vocab entropy, average sequence length, and number of tokens appears to diverge by ID method category. We observe the following (see figs. E.6 and E.7):

- Trends appear to be opposite for PCA/FisherS and the other ID estimators.
- For PCA/FisherS, ID generally correlates negatively to linguistic descriptors like average input length, vocab size, and vocab entropy.
- When significant, vocab size and entropy generally correlate positively to ID aggregates for estimators that aren’t PCA/FisherS.

ID and Linguistic Structure Beyond ESS (section 4.3), the increasing trend in ID/PPL for variants of wikitext, successively baseline $<$ permuted $<$ swapped $\lesssim$ random, also holds for virtually all ID estimators and model sizes (fig. E.5)– all but PCA/FisherS (not pictured in the figure), who estimate ID of all variants to be baseline $=$ permuted $=$ swapped $<$ random.

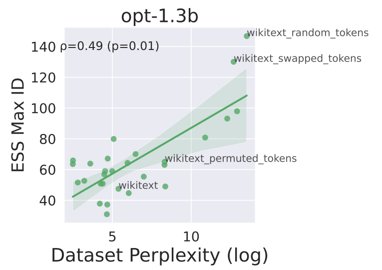

(a) ESS max ID vs. log-PPL

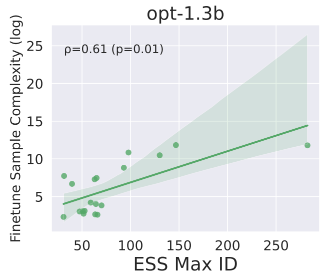

(b) ESS sample complexity vs. max ID

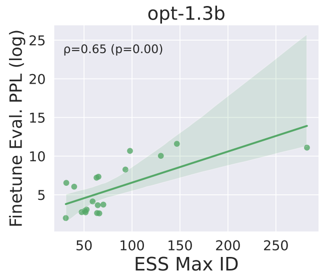

(c) ESS final PPL (log) vs. max ID

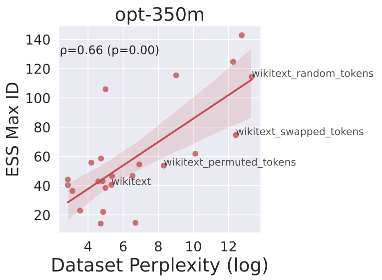

(d) ESS max ID vs. log-PPL

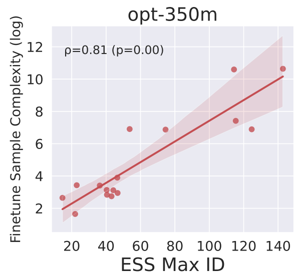

(e) ESS sample complexity vs. max ID

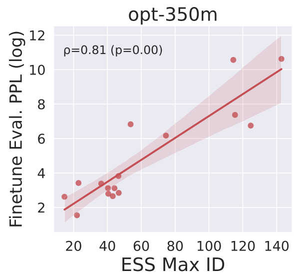

(f) ESS final PPL (log) vs. max ID

Figure E.3: For OPT-1.3b (top row) and OPT-350m (bottom row), max ID estimated with ESS is positively correlated to (a,d) dataset PPL (significant with $p \leq 0.01$ for both models); predicts ease-of-adaptation metrics (b,e) sample complexity (significant with $p \leq 0.01$ for both models); and (c,f) final evaluation PPL (significant with $p \leq 0.01$ for both models). Datapoints for wikitext and its perturbations are labeled for reference. The right two plots contain the subset of datasets tested that are suitable for a causal language modeling objective.

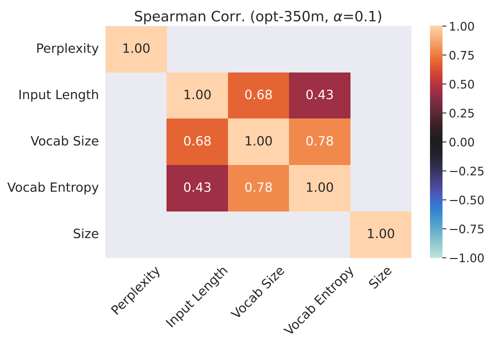

(a) OPT-350m data correlations

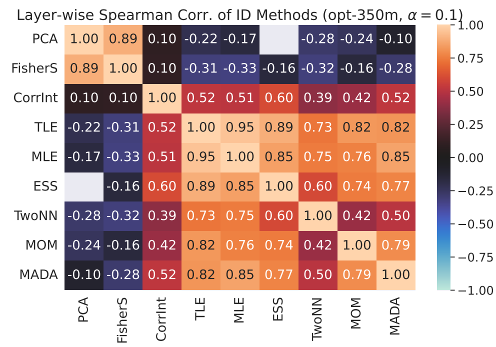

(b) OPT-350m ID correlations

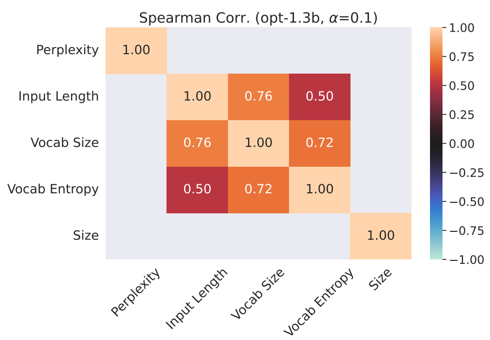

(c) OPT-1.3b data correlations

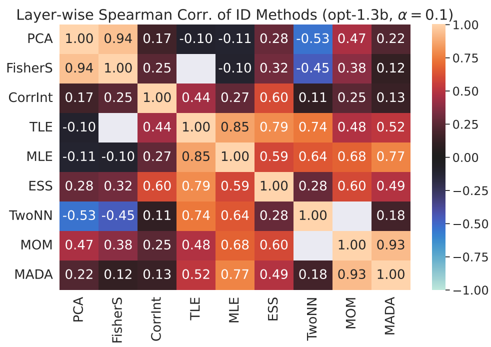

(d) OPT-1.3b ID correlations

Figure E.4: Data metrics Spearman correlations for left column (a) OPT-350m and (c) OPT-1.3b; and ID metrics Spearman correlations for right column (b) OPT-350m and (d) OPT-1.3b. Note the inter-correlations between shallow linguistic descriptors input length, vocab size, and vocab entropy for all model sizes, as well as the grouping of ID metrics into one block corresponding to NN-based methods (bottom right of each plot).

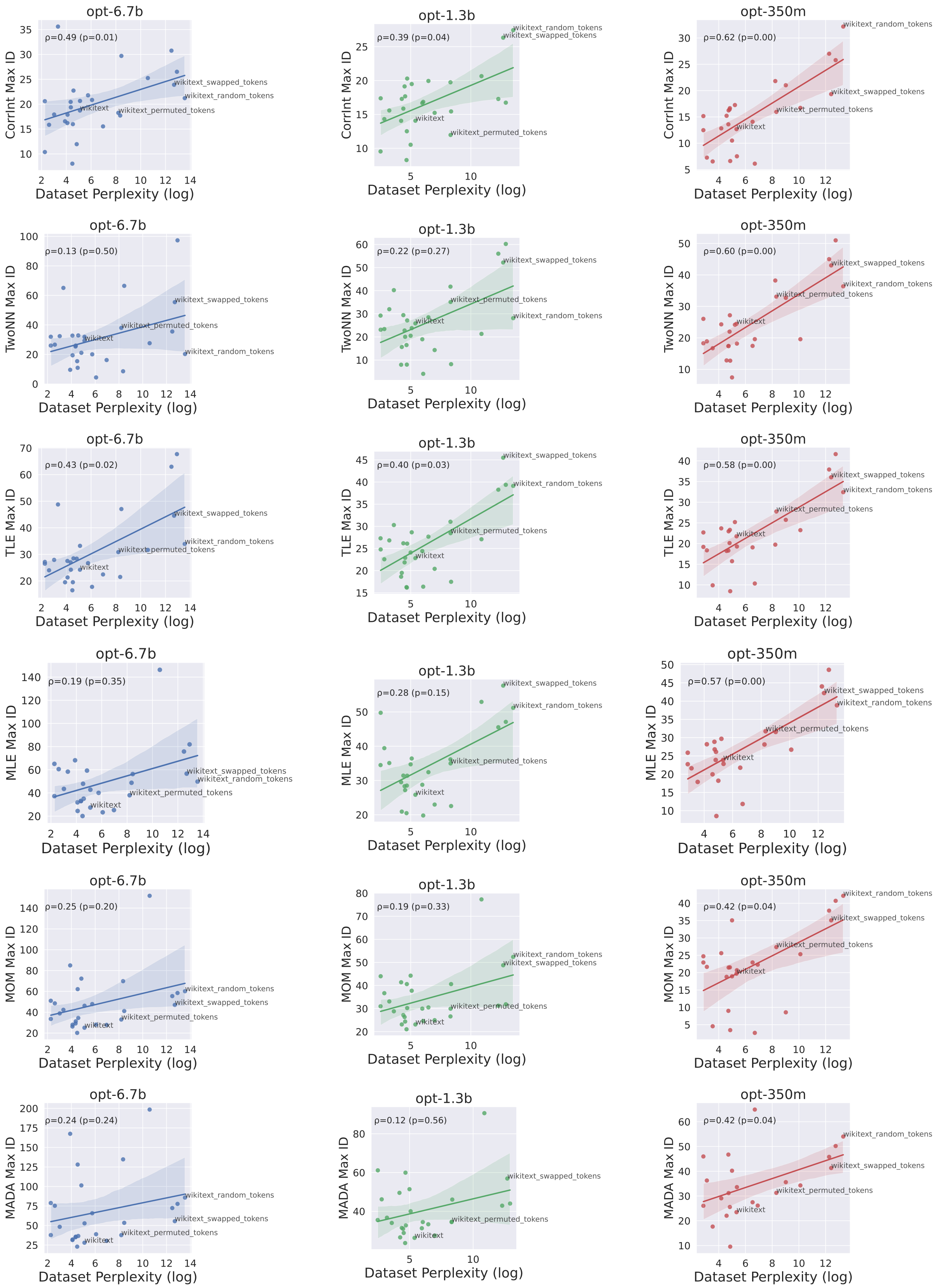

Figure E.5: For OPT-6.7b (left), OPT-1.3b (middle) and OPT-350m (right), and for all other ID estimators considered, we plot max ID vs. dataset PPL (log), labeling the points for wikitext. Across estimators and model sizes, we see a general trend that ablating linguistic structure increases ID as well as PPL, in the order of baseline $<$ permuted $<$ swapped $\lesssim$ random.

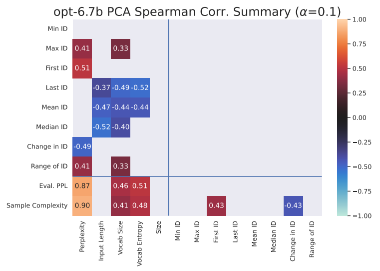

(a) OPT-6.7b, PCA

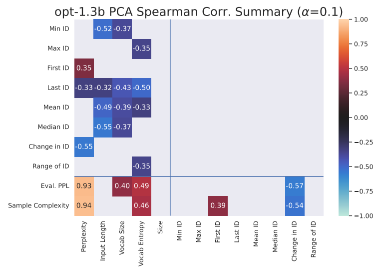

(b) OPT-1.3b, PCA

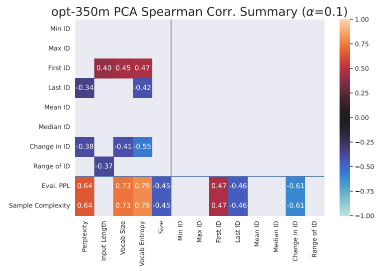

(c) OPT-350m, PCA

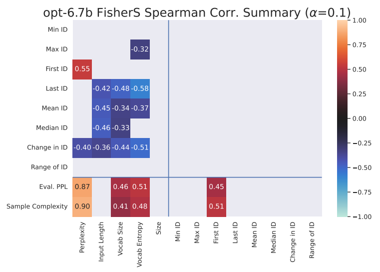

(d) OPT-6.7b, FisherS

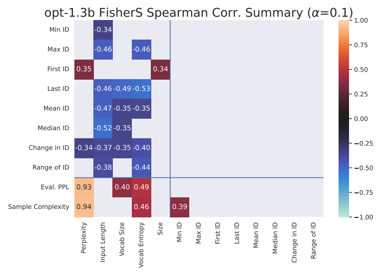

(e) OPT-1.3b, FisherS

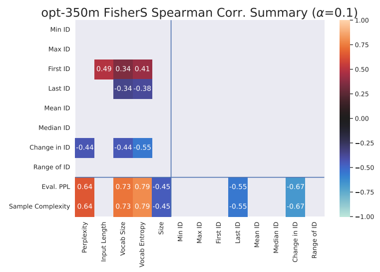

(f) OPT-350m, FisherS

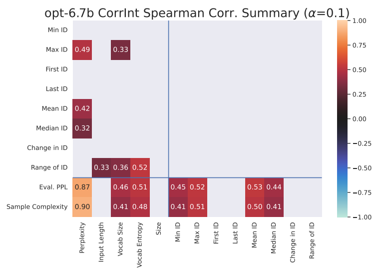

(g) OPT-6.7b, CorrInt

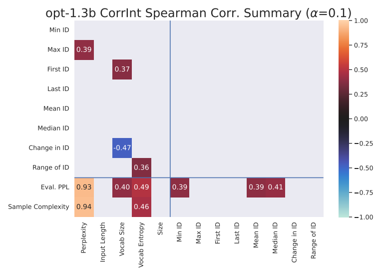

(h) OPT-1.3b, CorrInt

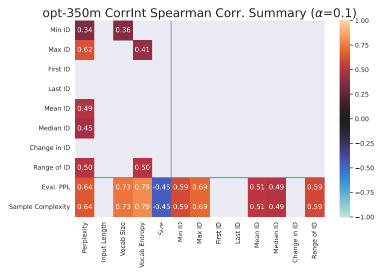

(i) OPT-350m, CorrInt

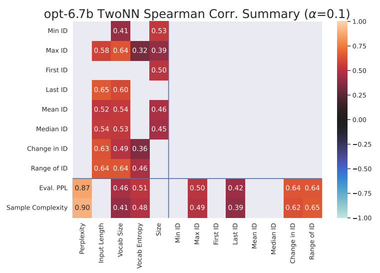

(j) OPT-6.7b, TwoNN

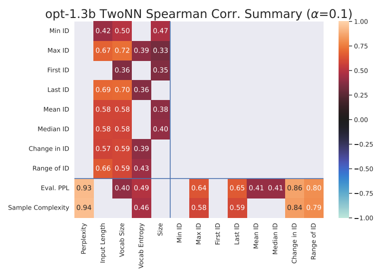

(k) OPT-1.3b, TwoNN

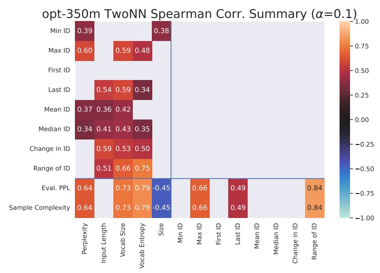

(l) OPT-350m, TwoNN

Figure E.6: Global ID Estimators: full panel of Spearman correlations for models (left to right columns) OPT-6.7b, 1.3b, and 350m. Each figure is a summary of Spearman correlations given a model and global ID metric, significant at $\alpha = 0.1$, between aggregated ID and data metrics (top left), ease-of-finetuning metrics and data metrics (bottom left), and ease-of-finetuning and ID (bottom right).

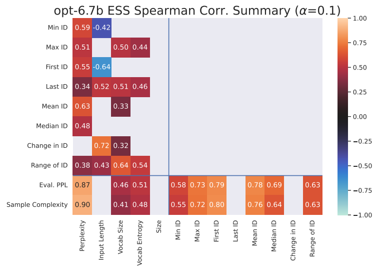

(a) OPT-6.7b, ESS

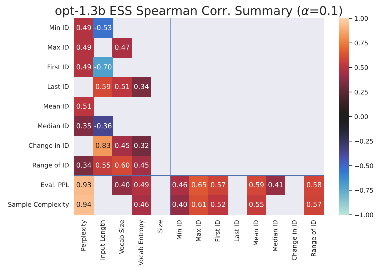

(b) OPT-1.3b, ESS

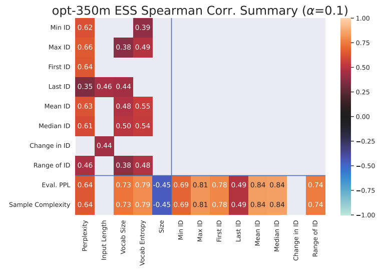

(c) OPT-350m, ESS

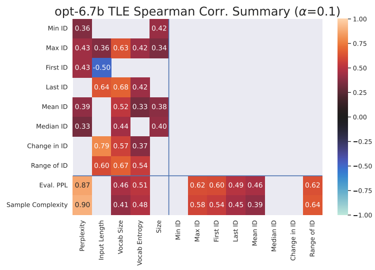

(d) OPT-6.7b, TLE

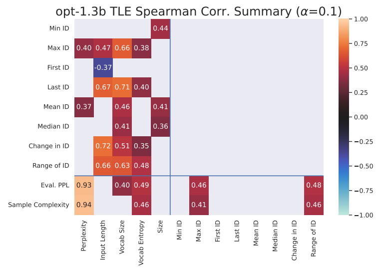

(e) OPT-1.3b, TLE

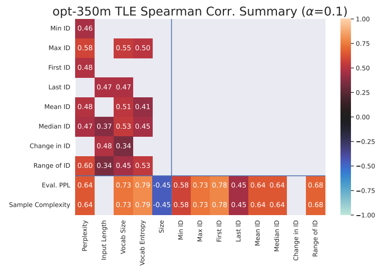

(f) OPT-350m, TLE

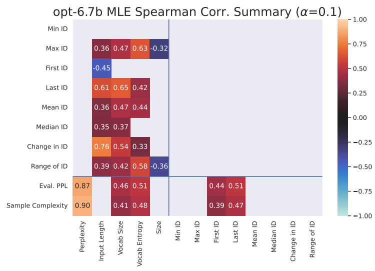

(g) OPT-6.7b, MLE

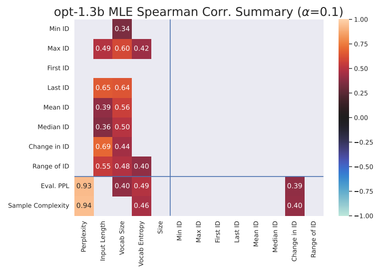

(h) OPT-1.3b, MLE

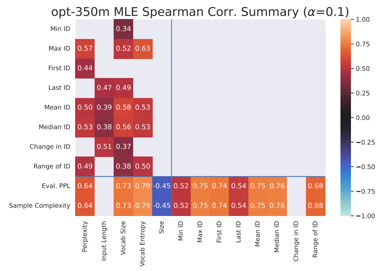

(i) OPT-350m, MLE

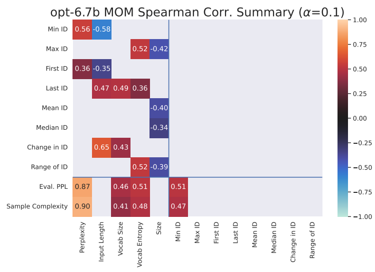

(j) OPT-6.7b, MOM

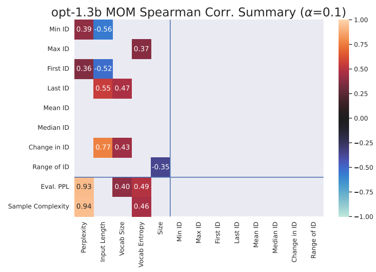

(k) OPT-1.3b, MOM

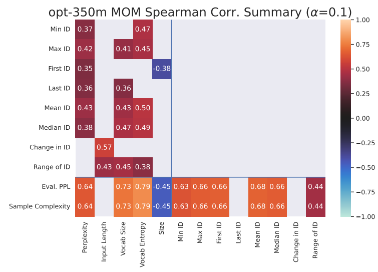

(l) OPT-350m, MOM

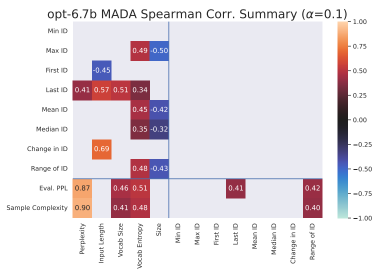

(m) OPT-6.7b, MADA

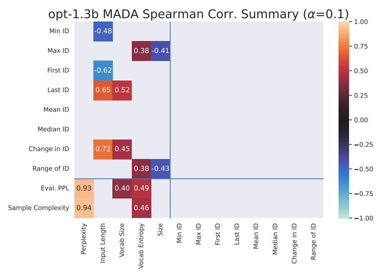

(n) OPT-1.3b, MADA

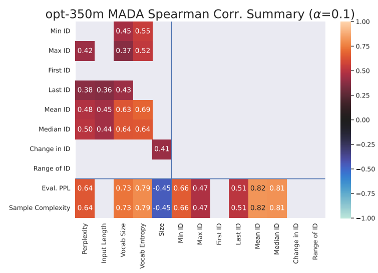

(o) OPT-350m, MADA

Figure E.7: Local ID Estimators: full panel of Spearman correlations for models (left to right columns) OPT-6.7b, 1.3b, and 350m. Each figure is a summary of Spearman correlations given a model and ID metric, significant at $\alpha = 0.1$, between aggregated ID and data metrics (top left), ease-of-finetuning metrics and data metrics (bottom left), and ease-of-finetuning and ID (bottom right).